CENTRO DE INVESTIGACIONES EN ÓPTICA, A.C.

"Pathogen detection via graphene oxide -based immunosensing: determination of bacteria in industrial samples of food"

MAESTRÍA EN CIENCIAS (ÓPTICA)

Asesor: Dr. Eden Morales Narváez

Estudiante: Mariana Denisse Avila Huerta

Agosto 2019

León, Guanajuato, México

"There's only one corner of the universe you can be certain of improving, and that's your own self."

– Aldous Huxley

To Victor and Lety that have always been my pillar and support.

ACKNOWLEDGMENTS

We acknowledge funding from the master fellowship given by CONACYT and the support from the grant given by SICES (Grant CMTEVAL-18-S01-03). Besides, we acknowledge the cooperation of "La próxima estación", which were our link with the industry; giving us the opportunity to be granted with this project. Also, because of the support of the general direction and quality control department who have been out technical support. Additionally, I specially acknowledge to Dr. Eden Morales who have advised and guided this work, and have been an excellent professor in every sense of the word. Evidently, without him and the group, "Biophotonic nanosensors", this work would have not been possible.

Personally, I would like to thank my family that have always support me and for giving me their unconditional love and respect in everything I do. Finally, I want to thank my friends who have been a really important piece of this stage, they have help me studying, accompanying me and motivating me in every difficult moment.

ABSTRACT

One of the major concerns of the food industry is the pathogenic bacterial contamination because it represents a risk to health of the consumer, it could cause several diseases and even death.[1] *E. coli* is a bacteria found in environment, foods and intestine of people or animals. Most E. *coli* strains are harmless but some others can cause serious food poisoning.[2–4] Currently, in food industry use culture-based assays on differential culture media to determination of pathogenic bacterial to ensure the food quality and the consumer safety. Despite this method is very accurate, it is time consuming and expensive. The development of biosensors and biosensing platforms results as an alternative for the reduction of time and cost of the pathogenic bacteria detection in food.[5] In this thesis, an optical biosensing platform based on Graphene Oxide (GO) is proposed aiming at detecting *E. coli* O157:H7, in food industry samples. The food industry samples were provided by "La Próxima Estación", a Mexican company dedicated to process frozen fruits and vegetables. The proposed biosensing platform reached a limit of detection (LOD) of 1.8 CFU mL^{-1} with a time response of 30 minutes. Also, it was demonstrated the selectivity of the antibody chosen as biorecognition element. Because of the matrix, for the real samples (vegetables such as spinach and cauliflower), it determined as positive or negative the presence of *E. coli* reaching a time response of 45 minutes.

Table of Content

Index of figures

Index of tables

Chapter 1. GENERAL INTRODUCTION

In this general introduction, it is briefly described the importance of the proposed biosensing platform as well as the general and particular objectives of the project. Also, first chapter highlights the justification of the project, giving information about the technics that currently are use in the food industry, specifically the culture-based methods and ELISA. Besides, an overview of the current developed of biosensing platforms that gives a scientific background is presented. In this manner, this chapter helps the reader to be contextualized about which is the problem, what does this work propose and what is the intention and the objectives of the project. This work proposed a system for bacteria determination in industry food samples, this system is based on Graphene Oxide (GO). This proposal is made with the intention of offering to the agro-food industry a faster, inexpensive, effective alternative of *E. coli* determination.

One of the major concerns of the food industry is the pathogenic bacterial contamination because it represents a risk to health of the consumer, it could cause several diseases and even death.[1] The bacteria that produce food contamination more usually are *Escherichia Coli* (*E. coli*), *Salmonella typhimurium, Listeria monocytogenes*, *Vibrio*, *Staphylococcus aureus*, among others.[6] An opportune detection of pathogenic bacteria in contaminated food is crucial to ensure the food quality and the consumer safety. The most commonly used methods for detection of microbial are culture-based assays on differential culture media.[7] This has been a continuous problem throughout the development of the food industry, because although this culture-based test provides very accurate results, it could take more than 48 hours to identify a pathogenic organism, that means, it is time consuming, more over these methods require analytical expensive instrumentation, highly trained personnel and a labor identification process.[5,7–9] In contrast we have the enzyme-linked immunosorbent Assay (ELISA) as one of the most conventional analytical techniques to detect microorganism. This analytical technique has been used for quality control check in several industries and it has some other applications in medicine and biotechnology. However, this result very expensive and time consuming because the assay requires a large number of reagents and at least 3 washing phases.[10]

The development of biosensors and biosensing platforms results as an alternative for the reduction of time and cost of the pathogenic bacteria diagnosis in food.[5] Also, this could represent an increase of selectivity and sensitivity of the detection of bacteria in food. In this thesis, an optical biosensing platform based on Graphene Oxide (GO) is proposed aiming at detecting *E. coli* O157:H7, a bacterium commonly found in contaminated food as mentioned earlier. Biosensors are measurement system used for the determination of the presence or absence of an analyte, the main parts of a biosensor are the biorecognition element that capture the analyte and give specificity to the sensing, and the transducer which transform a physical or chemical response to a signal that can be analyzed.[6] Antibodies are generally used as biorecognition element, antibodies are immune protection proteins produced by immune system cells when exposed to antigen such as pathogenic bacteria or viruses. These proteins are Y-shaped molecules and selectively bind with an antigen (analyte) due to their geometric compatibility as lock-and-key combination.[10]

An optical biosensor is a device that can detect biological or chemical responses and reported it as change in any optical signal that can be measured such as absorption, fluorescence, change in the refraction index, polarization, amplitude, phase, etc. Recently the use of nanomaterials for biosensing as transducer elements has become popular because it might improve the performance of this systems due to their unique combination of properties and biocompatibility. Furthermore, this allows for the

miniaturization of the sensors and devices with nanometer dimensions in order to acquire better sensitivity, specificity and faster responses.

General Objective

To develop a biosensing platform based on nanomaterials and their optical properties and interactions. This platform will allow the detection of *Escherichia coli*, to determine the presence of pathogenic bacteria in food. This platform will be used in agro-industrial samples, specifically provided by "La Próxima Estación", a Mexican company dedicated to process frozen fruits and vegetables.

Particular Objectives

1. To optimize the bionanoreagents concentration for the implementation the bionanotechnology proposal.
2. To characterize the analytical behavior of the platform proposed according to the limit of detection and the accuracy exhibited by the system.
3. To test the response of the developed platform using real samples provided by the company and compare these results with conventional tests (culture-based assays).

Justification

Outbrake pathogenic bacteria is the major cause of gastrointestinal diseases around the world, the main responsible of these diseases are *Escherichia coli* (*E. coli*), *Salmonella spp*., *Listeria monocytogenes*, *Staphylococcus aureus*, among others. Bacteria are commonly introduced to the human body by the intake of contaminated food. The food industry is responsible of guarantee quality and safety products to consumer, currently they verify that products are free of pathogenic bacteria using culture test which are time consuming and expensive.

"La Próxima Estación" is a company, that for over 30 years have been growing and processing frozen fruits and vegetables in the Bajío area of Mexico. They work to provide the world with healthy food that complies with the highest quality and hygiene standards, while supporting people, community and environment. Some of the products that they process are Broccoli, Cauliflower, Spinach, Carrot, Kale, Mango, Strawberry and Raspberry. This company are collaborating with this project, they spend more than 48 hours to assure the quality of the product, this cause a delay in product delivery. In this project, a biosensing platform intended for simple food analysis is developed. The developed platform is cost-effective and allows the reduction the time per test to determinate the presence or absence of *E. coli*, in this way it could potentially reduce delivery time by the company as well as guaranteeing the safety and quality of food.

Hypothesis

Biosensing platform proposed will get advantage of the quenching capabilities of the GO, using antibodies as biorecognition element and quantum dots as fluorophore will be able to determine the presence of bacteria. *E. coli* will be used as model analyte and if operating principle results convenient for this application then the biosensing platform could be expanded for other analytes in later works. Due to the use of only one antibody the test proposed to detect *E. coli* will keep selectivity of the commonly used immunoassay as ELISA, but with lower cost. Also, this sensing platform could reduce the time invest to determine contamination in a sample from 48 hours to 1 hour because of the properties of GO.

Background

Culture-based assays and Immunoassays

Microbial culture are methods to determine the presence, type and abundance of an organism in a sample tested. This technic consists in multiply the microbial microorganisms, making a good environment for reproduction with a culture medium.

"La Próxima Estación" uses the 3M™ Petrifilm™ *E. coli* / Coliform Count (EC) Plate, which is a culture medium system ready to use that already contains the medium to grow the bacteria and a colorant that facilitates the count of the colonies formed. With these plates they do this process in three steps, inoculate, incuba and interpret and it takes around 48 hours

An immunoassay is a biochemical test used to detect the presence of a specific analyte mainly used in medic diagnosis, food industry and control environment. An analyte is everything that could be measured in a laboratory test such as proteins, peptides, enzymes, viruses, pathogenic bacteria, among others. This test used an antibody for analyte binding, also immunoassays require many different reagents and washing steps. Enzymes are one of the most popular labels used in immunoassays, the immunoassays that employs enzymes as label are called Enzyme Linked Immunosorbent Assay (ELISA).[11,12] The enzymes induce a color change in presence of a chromogen which occur in presence of the target analyte, in the Fig. 1.1 is shown a schematic representation of the sandwich ELISA and all the reagents required for the assay.

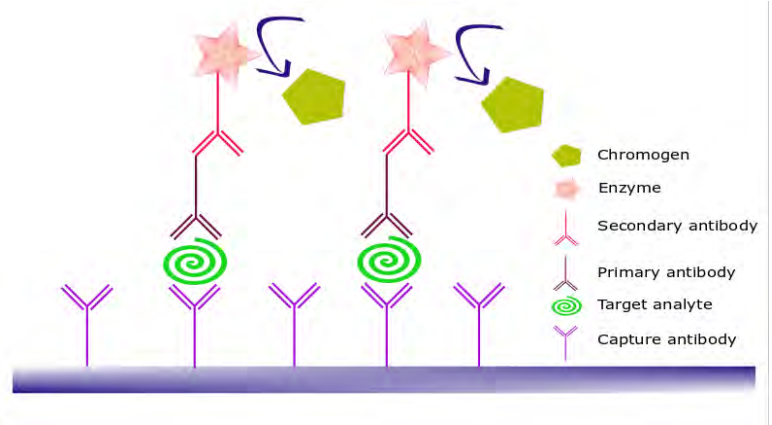

Figure 1.1. Sandwich ELISA

Biosensing platforms based on graphene oxide (GO)

The discovery of the exceptional optical and electronics properties of GO and its heterogenous structure have allowed the development of biosensors based on this nanomaterial, attempting in this way to improve the performance of sensors; the structure and the properties of GO are explained in more detail later. Some of these biosensors get advantage of the quenching capabilities of graphene oxide, using the fluorescence of some fluorophores and a biorecognition element. Over the last decade, the field of food nanosensors has grown exponentially, this nanosensors are suitable to many types of analytes such as small organic molecules, biomolecules or food-borne pathogens.[5]

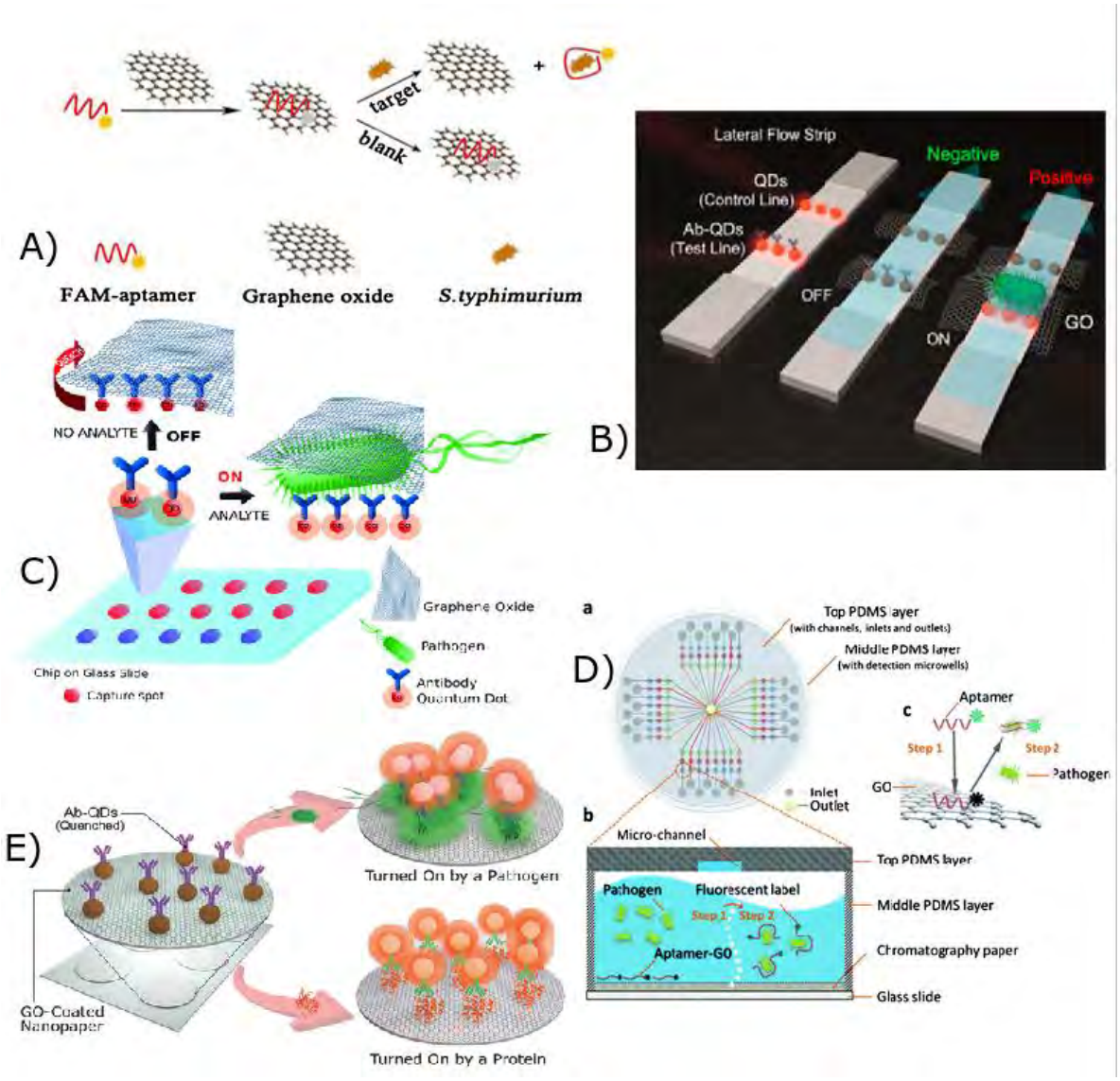

Figure 1.2. Biosensors based on GO for bacterial detection. A) Aptasensor for Salmonella detection. Adapted with permission.[13] Copyright 2014, Springer Link. B) LFA with GO as revealing pathogen agent. Adapted with permission.[14]Copyright 2015, American Chemical Society. C) Operational concept of GO as pathogen revealing agent in a microarray. Adapted with permission.[15] Copyright 2013, Wiley-VCH. D) Schematic of the PDMS/paper hybrid microfluidic system for one-step multiplexed pathogen detection using aptamer-functionalized GO biosensors; (a) Microfluidic biochip layout, (b) principle of the one-step 'turn-on' detection. Adapted with permission.[16] Copyright 2013, Royal Society of Chemistry. E) GONAP. Adapted with permission.[17] Copyright 2017, Wiley-VCH.

Herein, a brief overview of this type of biosensing systems is highlighted. Duan and colleagues reported an aptasensor for detect *Salmonella typhimurium* using a GO platform and a FAM-labeled aptamer, a schematic representation is shown in Fig. 1.2 A). In optimum condition the platform can show a linear response with bacteria concentration between 1×10^3 to 1×10^8 CFU mL^{-1} and a limit of detection of 100 CFU mL^{-1}.[13] Another example of this progress is the system developed by Morales et al. which uses GO as Pathogen revealing agent and an antibody-quantum dot probe in a microarray

platform reaching a limit of detection of 5 CFU mL^{-1} giving a digital response (ON/OFF) in a short period of time, the determination takes about 75 minutes, in Fig. 1.2 C) it's found the operational principle of this biosensor.[15] Another trend that is taking importance in the bacteria sensing field is the used of solid phase substrates such as nanopaper or biofunctionalized glass. Zuo reported a microfluidic glass biochip that can be multiplexed for simultaneous detection of two pathogens, *Staphylococcus aureus* and *Salmonella enterica* which is shown is Fig. 1.2 D), and reached a limit of detection of 11 CFU mL^{-1} with a time of detection of 10 minutes.[16] Also, a paper-based Lateral Flow strip assay has been developed by Morales-Narvaez et al. and by other research groups as reviewed by Luo and colleagues.[1] Morales-Narvaez achieved a limit of detection of 10 CFU mL^{-1} in standard buffer and 100 CFU mL^{-1} in bottled water and milk with the aforementioned lateral flow strips without the need of a second antibody as it can see in Fig. 1.2 B).[14] Cheeveewattanagul also has worked in a Graphene Oxide-Decorated Nano paper (GONAP), Fig. 1.2 E), in which a limit of detection of 55 CFU mL^{-1}in standard buffer is reached. Furthermore, the authors test real samples such as poultry meat and river water reaching a limit of detection of 65 y 70 CFU mL^{-1}, respectively.[17]

Chapter 2. THEORETICAL FRAMEWORK

This chapter explains all the necessary concepts to understand how the proposed biosensing platform works. First of all, it is introduced a general explanation about biosensing systems. It is listed and explained the principal components of a biosensors. Also, it is pointed the components used to develope the proposed platform. Then, it is exposed a phenomenon called FRET, that is crucial for the performance of the biosensing platform. Moreover, in this chapter a full section is dedicated to describe some nanomaterials and its properties, particularly graphene oxide and quantum dots. As mentioned before, this optical biosensing platform is based on GO, that is why it is so important to describe the properties and advantages of using this nanomaterial. Once explained all this concept, it is described the operational principle of the proposed biosensing platform. Finally, there is an overview of the model analyte used, this is *E. coli*. Also, in this final section of the theoretical framework, the complications of the intake of food contaminated with *E. coli* are discussed.

Biosensing

Biosensors are devices utilizing the specific interaction between a biological element (biosensing agent) and a target molecule (analyte). Such a specific interaction is exploited to determine the presence of the analyte in a sample; this biorecognition phenomenon is converted into a physical signal. [6,18,19] Biosensors have had an exponential growth over the las decades, this because biosensors are a great option to monitor and determine the presence of an analyte in several fields such as clinical diagnostics, food industry, environmental monitoring and any area which requires reliable and quick analysis. Biosensors must gather important features including, [18]

1. Selectivity: capability to select and measure only the analyte even in presence of other species in the analyzed sample.
2. Suitable limit of Detection (LOD): minimum concentration of the analyte that can be detected.
3. Lifetime: functional time of the biorecognition element before it starts a degenerative process.
4. Response time: speed in the kinetics of the reaction.[18]

As mentioned in previous chapter, the key components of biosensors are the biorecognition element and the transducer.[18] These elements and some specifications of it are discussed below.

Biorecognition element

The biorecognition element specifically interacts with the analyte and determines the selectivity of the developed biosensing system. The targets can be proteins, enzymes, drugs, pesticides, viruses or bacteria.[5,18] Molecular interactions between recognition elements and analytes can be based on different interactions such as hydrogen bonding, metal coordination, hydrophobic forces, van der Waals forces, π-π interactions and electrostatic interactions. Antibodies are the most common recognition elements used in immunobiosensors.

Antibodies

Antibodies are soluble proteins produced by plasma cells from the immune system. Antibodies neutralize viruses or mark antigens by binding them for destruction via phagocytosis or complement lysis. They are very specific and have very high affinity to bind the corresponding antigen. This is crucial for biosensing, specially to detect antigens present in low concentration levels. Biosensing selectivity and specificity are given by the employed antibodies (or the biorecognition element used). Antibody types can be classified as polyclonal and monoclonal antibodies. Polyclonal antibodies are able to recognize multiple segments onto the same antigen, whereas the monoclonal counterparts only bind with one unique segment of the analyte.[19,20] The antibody to be employed may depend on the

final application. For example, the polyclonal due to its high affinity against the antigen is recommended to ELISA assay. Also, polyclonal antibodies are less expensive, are easy to attach to a fluorophore and have a faster response to capture de target.[20] Moreover, monoclonal antibodies are recommended to use for develop of therapeutic drugs, because it requires large amounts of identical antibodies.[20,21]

Transduction system

The transducer detects a signal produced by the analyte and the biorecognition element, then, it transforms the signal so as to measure a physical, chemical, electrical or optical signal. [18,19] Transductions can be classified according to the signal produced to be measured, the most commonly used are optical and electrochemical. Hereupon, it is briefly described the optical transduction system and fluorescence-based transduction.

Optical transduction

The interaction between light and matter can derivate in absorption, transmission, reflection, scattering, emission of radiation or a change in refractive index or polarization. These interactions allow to acquire information of the system that is being studied. The proposed platform uses an optical transducer specifically used a fluorescence transducer. [19]

Fluorescence-based

Because of its high sensitivity, fluorescence is a very common technique in optical biosensing, sometimes using fluorescence-labelled binding proteins such as antibodies. Fluorescence belongs to a set of optical phenomena called photoluminescence that occurs when a fluorescent atom absorbs a photon of high energy, from an external light source, which excites an electron from the ground state to a higher energy state. Then, the excited electron decays to a lower energy state while emitting the remaining energy as a photon with lower energy than the absorbed photon, it means with a larger wavelength. [19,22–24] Fluorescence molecules are usually used as tags or reporters, these molecules can be attached to other molecules, such as antibodies for detection. [22] Fluorescence-based biosensors can exploit a physical phenomenon called Fluorescence Resonance Energy Transfer (FRET) which is explained below.

Fluorescence/Föster Resonant Energy Transfer (FRET)

FRET is a physical phenomenon that involves two molecules, one called the donor and other called the acceptor. In this process, excitation energy is transferred from a donor fluorophore to an acceptor molecule. The donor has to be on an excited state and the acceptor molecule should be on a ground state and is generally observable around 6-10 nm, Fig. 2.1 is an energy level diagram that represent

schematically the phenomena. Another feature for FRET to take place is that the donor molecule emission spectrum has to overlaps the absorption spectrum of the acceptor. Due to dipole-dipole interactions that are produced between donor and acceptor the transfer of energy can happen without the emission of a photon. The factors that determine the index of energy transfer include spectral superposition of emission spectrum of donor and absorption spectrum of acceptor, the distance between acceptor and donor, the quantum yield of the donor and the relative orientation of the transition dipoles of donor and acceptor. Typically, the distance between the donor and the acceptor which gives more efficiency is in the range 20 to 60 Å, this distance is commonly called Föster distance(R_0). The rate of the energy transfer can be described by:

$$\kappa_T = \frac{1}{\tau_D}\left(\frac{R_0}{r}\right)^6.$$

Where: τ_D is the decay time of the donor and r is the distance between donor and acceptor.[25–28] FRET phenomenon involving nanomaterials such as graphene related materials (as acceptor) will be described below.

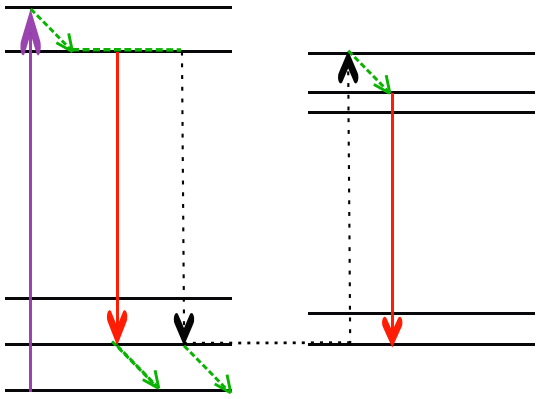

Figure 2.1. Energy level diagram

Nanomaterials

To take advantage of FRET, is necessary to find the best molecules to perform as donor and as acceptor. Optically active nanomaterials exhibit properties than allow to exist this phenomenon efficiently.

Nanotechnology is a technology operating at the nanoscale, that is, form 1 to 100nm, it has several application in the real world in different fields such as, energy, environment, food, agriculture and of course in photonics, biomedicine and health care.[29,30]

Nanomaterials are nanoscale materials, where at least one dimension in their structure is less than 100nm. At this scale properties of materials can be extremely different from those materials at larger scales. With this change in properties, the nanostructures could perform with no predictable behavior in terms of what they exhibit at the macroscale. Also, this reduction of dimension from a larger scale to a nanoscale allows generation of novel properties due to dominance of size confinement, distribution and morphology, interfacial phenomena and quantum effects.[29]

Commonly, nanostructure materials exhibit unusual chemical and physical properties such as catalytic, structural, electronic, magnetic, and optical among others. These nanomaterials attached to a biorecognition element can be a key component of a Nano-biosensor.[31]

Classification

The nanostructure materials can be classified by dimension, that is 0D, 1D and 2D. Any of these together may form a 3D material.[32] Herein, it is described some of these nanomaterials in agreement with this classification. Within zero dimensional (0D) materials can be mentioned mainly gold nanoparticles (AuNP), magnetic nanoparticles (MNP) and quantum dots (QD). Any of these functionalized may be biocompatible and useful as biomaterials or for biological systems and biomedical applications. Regarding one-dimensional (1D) materials, we find nano wires and carbon nanotubes (CNTs). Finally, two-dimensional nanomaterials (2D) include, molybdenum disulfide (MoS_2), black phosphorus and specially graphene. [33–36]

Quantum Dots

Quantum Dots (QDs) are fluorescent nanocrystals, usually with spherical shape with 2 to 10 nm in diameter. Biofunctionalized QDs are commonly used for biological applications such as bio-detection. QDs may include a core shell configuration and finally the biofunctionalization with a biomolecule as shown in Fig. 2.2.

QDs band gap is tunable according to the size of the particle. Therefore, optical properties, including emission wavelength, can be tuned by regulation of the size. QDs are brighter, almost an order of magnitude larger, more stable and show narrower and more symmetric emission spectra than conventional organic dyes and fluorescent proteins. Also, QDs have high quantum yields and high resistance to phobleaching and chemical degradation. [37,38]

QDs are used as fluorophores in the proposed biosensing platform, they have Cadmium selenide (CdSe) core, Zinc sulfide (ZnS) shell, polymer coating and were functionalized by the conjugation with streptavidin. Nowadays, different QDs are available for purchase from some laboratories, the QDs that were used for this project were obtain form ThermoFisher as QD 665 Streptavidin conjugate.

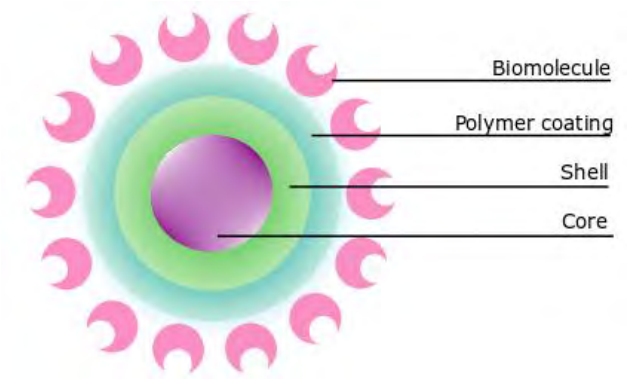

Figure 2.2 Schematic functionalized Quantum Dot

Graphene Oxide (GO)

Due to the attractive mechanical, electrical, thermal, and optical properties of GO that have been discovered, GO has become an interesting topic in the scientific community. GO exhibits very interesting optical properties that can be useful to develop new science and technology. [39–41]

An important application of GO can be focused on biosensing, specifically with optical transduction because of its novel optical properties which will be discussed in this chapter; However, GO has many other applications such as nanoelectronics devices, photovoltaic cell fabrication, energy storage and catalysis, biomedical application to name a few.[42,43]

GO Structure

Graphene oxide (GO) is a monolayer of Graphite oxide.[44] GO has an atomic distribution similar to graphene, which is described as a one atom thick planar sheet of carbon atoms ordered in a hexagonal arrange in tow dimensions, but decorated with oxygen-containing groups,[43] see Fig. 2.3. The presence of these oxygen-containing groups (carboxyl, hydroxyl and epoxy groups) determine the oxidation degree that give hydrophilic properties and allow the formation of stable aqueous colloids well as functionalization capabilities.[39,43]

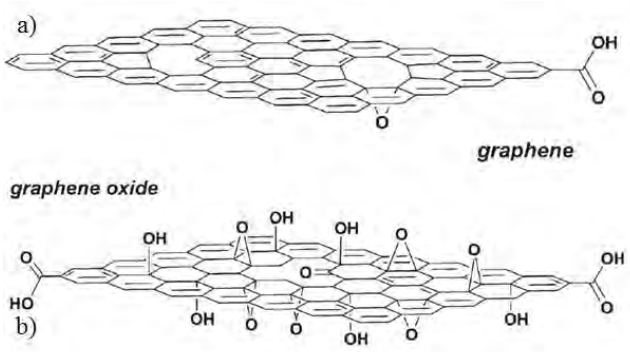

Figure 2.3 Graphene and Graphene Oxide structure. Adapted with permission.[45] Copyright 2010, Wiley-VCH.

The main GO characteristics that define this nanomaterial are the number of layers, lateral size and oxidation degree, for optical bio sensing application is crucial to choose carefully these features because they give specific optical properties such as of as absorbance, optical transparency, and photoluminescence quenching abilities.[46]

Optical Properties

1. *Fluorescence*

   Lack of band gap in graphene suggests that fluorescence should not be possible, only if is induced by phonons. However, given the heterogenous atomic and electronic structure GO, this graphene derivative exhibits from NIR to ultraviolet fluorescence. This fluorescence is produced from recombination of electron-hole pairs in certain electronic states instead of the band edge transition that take place in the typical semiconductors.[47]

2. *Fluorescence quenching capabilities*

   Although GO exhibits fluorescence properties, GO can also quench fluorescence. In fact, GO is able to quench any fluorescence wavelength by energy transfer. This is possible because Graphene and its derivates are optically omnivorous, that is, these materials can absorb in almost all the electromagnetic spectrum. This fluorescence quenching ability is determined by the number of layers of GO and its oxidation degree, the more oxidized the less efficient in terms of quenching capability. This quenching effect is originated by Föster Resonance Energy Transfer (FRET), or no radiative dipole-dipole coupling, this FRET is described above.[39,47] However, using GO as FRET acceptor the efficiency exhibited is higher than the general case due to the rate of the long-range resonance energy transfer in dependence of $(R_0)^{-4}$. It is estimated that GO as quencher can be observable up to a distance of about 300 Å.[48,49]

Besides quantum dots, another nanomaterial that is necessary for this project is GO, actually without these quenching capabilities described above the platform proposed could not work. The GO used is described by the provider as "Single layer Graphene Oxide, that incorporates oxygen-containing chemical groups on graphene basal plane. It is dispersible in water and available in 5 mg mL^{-1}. It possesses polar functional groups and it is electrically and thermally insulating. Its lateral size is around 500 nm and its thickness accounts from 0.35 to 1 μm".

Conjugation

As mentioned in section 2.1.2, fluorescence-based biosensors require the attachment of a fluorescent molecule, commonly called fluorochrome, to a biological molecule such as an antibody. In this manner the fluorochrome performs as a reporter or a label and the antibody as a biorecognition element. Several strategies to conjugate (attach) these two molecules can be employed, which can be classified in two types: Covalent and Noncovalent.[21,50] Noncovalent methods generally are based on the affinity interactions that could be easily broken, but, there is an exception to this rule, Streptavidin/Biotin pair. Although the interaction between streptavidin and biotin is noncovalent, the bond is strong enough to be consider as stable in the long term.[50,51]Covalent modes are also used to bind bio-functional groups such as amino, hydroxyl and carboxyl groups. Usually, covalent conjugations require bifunctional linkers or mediator linkers to form the complex. This method can be used, for example, to conjugated antibodies and nanoparticles. [52,53]

Streptavidin/Biotin interaction

Biotin binding to streptavidin is one of the strongest noncovalent biological interactions in nature.[21] Biotin-Streptavidin bond is greatly used for in vitro diagnosis assays because these assays require the formation of an irreversible very specific bond between biological macromolecules. The high affinity between this pair is a result from many factors such as the formation of multiple hydrogen bonds and van der Waals interactions. Also, the ordering of the surface of the streptavidin allows biotin to stay under the streptavidin interior, giving it the strength of the bond .[54]

The Studied Biosensing Strategy: Operational Principle

Upon explain all the required concepts to described and understand the behavior of the proposed biosensing platform to detect bacteria, above is a description of its operating principle and the model analyte.

The proposed biosensing platform is a system based on optically active nanomaterials. Consequently, it uses an optical transduction mechanism. This system operates under the FRET that was mentioned above; As donors it is used QDs and as acceptor or quencher GO. Morales-Narváez reported the

interaction between the absorbance spectra of several carbon materials and the emission of QD, in this report it is clear that GO is the one which exhibit better quenching capabilities than the other carbon materials (graphite, carbon nanotubes and nanofibers). Fig. 2.4 shows the overlapping between the absorbance and emission spectra.[25]

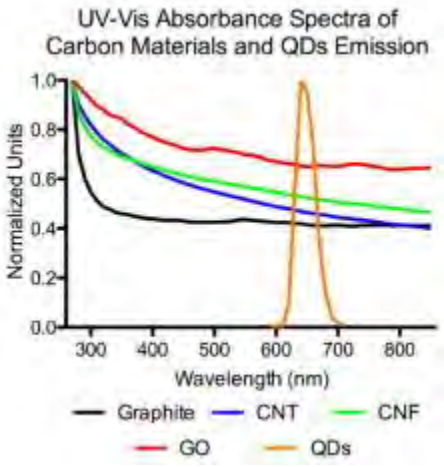

Figure 2.4. Overlap Between Absorbance Spectra of Carbon materials and QD's emission. Adapted with permission.[25] Copyright 2012, Elsevier.

It is necessary for the platform to have the GO as a base to perfom as quencher of fluorescence, GO is attached onto the bottom of a polystyrene microwell. This attachement between GO and the polystyrene well takes place because of electrostatic interactions, GO is postively charged and the polyestiren is negatively charged, this allows the interaction and the stability of this interface.

Besides, as recognition probe it is used an antibody attached to a QD, the antibody gives selectivity to the assay and QDs serve as a label. Fig. 2.5 is a schematic representation of this probe. The way to achieve the conjugation between the antibody and the QD is through the noncovalent bond between streptavidin and biotin that was mention above. It means, the antibody is attached to a biotin and the QD is attached to a streptavidin, so the streptavidin and the biotin make a natural and strong bond between Antibody and QD making a strong and big recognition probe (~20nm).

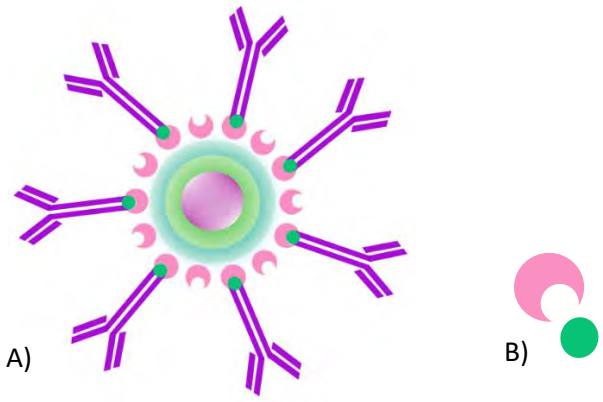

Figure 2.5. Ab-QD conjugation. A) Ab attached to a QD. B) Streptavidin/Biotin bond

As mentioned above, QDs operate as donor and GO as acceptor, so transfer of energy can ocur and allows to detect an analyte. The exchange of energy happens depending on the distance between the donor and the acceptor. Therefore, if the distance among the two components is reduced in the order of the Föster distance, the QDs will experiment a quench of fluorescence. But, if the distance between them is larger that Föster distance, it will not be energy transfer, and the QDs will keep its fluorescence. In absence of the analyte (bacteria), the probe will not link to any molecule and the probe will be able to go to the bottom and get closer to the GO. Herein, the GO will absorb the energy recived from the QDs and quench its fluorescence. Whereas in prescence of analyte, the bacteria will get between the probe and the GO because a bacterium will attach to Ab-QDs complexes. This causes that QDs and GO get apart in a larger distance, so, QDs can exhibit virtually normal fluorescence. Summing up, in absence of bacteria QDs fluorescence will quench; however, in prescence of bacteria QDs will emit fluorescence. Fig. 2.6 describes the behavior of the biosensing platform. Herein, the model analyte is *E. coli*. This bacteria measures around 2µm, that means that the distance between QDs and GO in the prescence of bacteria will be bigger than 2µm. The following section highlights related to *E. coli* infection.

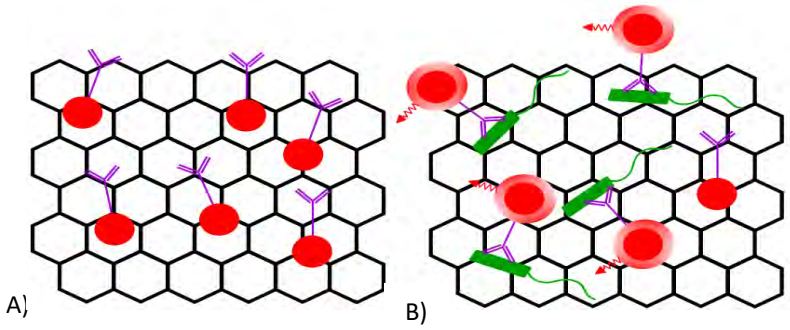

Figure 2.6. Schematic representation of detection system. A) In absence of E. coli, quenching fluorescence. B) In presence of E. coli Fluorescence recovery

Escherichia coli (E. coli)

E. coli is a rod shape, non-spore-forming, Gram-negative bacteria that moves by a flagella.[55,56] This bacteria is found in enviroment, food and intestine of people and animals. Most *E. coli* strains are harmless but some others can cause serious food poisoning. *E. coli* that produces Shiga toxin is the one that causes diseases and is called “Shiga toxin-producing" *E. coli* (STEC). The most common serotype related to public health and food safety is *E. coli* O157:H7; however, other serotypes are also involve sporadic cases and outbrakes. [2–4] According to World Health Organization (WHO), *E. coli* O157:H7 is transmitted to humans by consuming contaminated food such as undercooked meat primarily through consumption of contaminated foods, undercooked products such as meat and milk and cross contamination. Also, the outbrakes releted to intake of contaminated fruits and vegetables (including sprouts, spinach, lettuce, coleslaw, and salad) has been increasing. Fruits and vegetables contamination may be due to contact with faeces from domestic or wild animals at some stage during cultivation or handling. Contagion from person to person is an importan mode of transmission. Some symtoms of disease produced by *E. coli* strains are fever, vomiting, abdominal cramps and diarrhea; althoug most of the patients recover whitin 10 days, in a small proportion of patients (10%) the infection may lead to a life-threatening disease, such as haemolytic uraemic syndrome (HUS) with a lethality rate around 3-5%. Some others may have renal or neurological complications.[3]

Chapter 3. EXPERIMENTAL METHODS

This chapter explains the methodology followed for the development of the proposed biosensing platform. This experimental methodology can be roughly summarized in four points: 1) Bionanoreagents optimization, 2) Analytical characterization, 3) Selectivity test and 4) Real sample test. In addition to the punctual explanation of these mentioned points, this section gives information related to the reagents used and its respective suppliers. In addition, as part of reagents, the buffer preparation is also described. Then, it is included a brief description of the equipment used as well as its main characteristics. Details on quantities or concentrations of the involved reagents are discussed in chapter 4 as part of the obtained results.

Reagents

All the information of the reagents used for the proposed system were provided by the supplier, according with these specifications the reagents were selected and purchased and carefully handled. Table 3.1 presents the provider of each reagent.

Table 1. Supplier of reagents

Reagent	Supplier
Graphene Oxide	Anstrong Materials
Quantum Dots 665 Streptavidin conjugated	Life Technologies
Anti-E. coli antibody (Biotin)	abcam
PBS	Sigma-Aldrich
BSA	Sigma-Aldrich
Tween 20	Sigma-Aldrich

Buffers

Buffers are solutions that contain a mixture of a weak acid and its conjugated base to maintain pH which prevents enzymatic changes and avoid ionic changes.[57,58]

Phosphate Buffered Saline (PBS) was used to perform dilutions of different reagents such as the sample and probe dilutions. Besides, PBS is used as the blank or control sample. It is prepared with 200mL of Milli-Q water and one PBS tablet from Sigma-Aldrich. PBS-Tween (PBST) is PBS with 0.05% of Tween 20 (v/v), it is used for washing steps that involve removal of unbound molecules such as antibodies. Blocking Buffer is prepared with PBS by adding 5% of milk powder (w/v) and 0.005% of Tween 20 (v/v) and it is used to block free binding sites. Immunobuffer is used to promote Ab-QD conjugation or immunolabeling, this is because this buffer facilitates interaction between biotinylated antibodies and streptavidin-QD.[59,60] It is prepared using PBS supplemented with 0.5% Tween 20 (v/v) and 1% Bovine Serum Albumin (BSA) (w/v). This buffer needs storage at 4-8°C

Equipment

Fluorescence spectrometer is the main equipment required in this approach. Although Cytation 5 by Biotek has several functions such as fluorescence microscopy, for this application it is only used as fluorescence intensity reader and Time Resolved Fluorescence measurer, using the software Gen5™. In Table 3.2 includes the most important technical details of the reader and Table 3.3 highlights technical details of Time resolved Fluorescence. Because of the use of QD's, the excitation wavelength needed is 360nm and the emission wavelength read is 665 nm.

Table 2. Cytation 5 Thecnical details: Fluorescence intensity.[61]

Cytation 5 **Cell Imaging Multi-Mode Reader** ***Technical details: Fluorescence intensity***	
Light source	Xenon flash
Detector	PMT for monochromator system PMT for filter system
Wavelength selection	Quad monochromators (top/bottom) Filters (top)
Wavelength range	Monochromators: 250 - 700 nm (850 nm option) Filters: 200 - 700 nm (850 nm option)
Monochromator bandwidth	Variable, from 9 nm to 50 nm in 1 nm increments
Dynamic range	7 decades
Sensitivity	Filters: Fluorescein 0.25 pM (0.025 fmol/well, 384-well plate) Quad Monochromator: Fluorescein 2.5 pM (0.25 fmol/well, 384-well plate) - top Fluorescein 4 pM (0.4 fmol/well, 384-well plate) - bottom
Reading speed (kinetic)	96 wells: 11 seconds 384 wells: 22 seconds

Table 3. Cytation 5 Technical details: Time resolved fluorescence.[62]

Cytation 5 **Cell Imaging Multi-Mode Reader** ***Technical details: Time Resolved Fluorescence***	
Light source	Xenon flash
Detector	PMT
Wavelength selection	Quad monochromators (secondary mode) Filters (top)
Wavelength range	Filters: 200 - 700 nm (850 nm option)
Sensitivity	Filters: Europium 40 fM (4 amol/well, 384-well plate) Monos: Europium 1200 fM (120 amol/well, 384-well plate)

Bionanoreagents optimization

Bionanoreagents optimization aims at achieving the best performance of the proposed biosensing platform generally using the least possible amount of material. It is obtained by finding the lower concentration of reagents that provided the best performance. (Bio) nanoreagents to be optimized are: GO, QDs and Anti-E. coli Antibody (Ab). According to the hypothesis and the theory, the best performance is reached when in absence of E. coli, the system shows the maximum quenching of fluorescence but in presence of E. coli, experiments the maximum fluorescence emission.

Optimization of the Ab-QD probe (procedure)

The chosen strategy to define a first approach of conjugation optimization (probe optimization) was to set fixed Ab concentration (100 µg mL^{-1}) and examine different QD concentration in a competitive assay. Firstly, to determine a proper concentration of QD, it was deposited 100µL of Ab in the well and incubated overnigth at 4°C. After that, it was needed three washing steps with PBST. Then, it was deposited 100µL of Blocking Buffer to cover all the rest of the surface and the plate was places on the shaker for 30 minutes with 650 RPM at room temperature. The blocking buffer was retired and five washing steps were performed with PBST. At this point, all the surface is cover with Ab and the free spaces are cover with the casein present in milk powder of the Blocking Buffer. The schematic representation in Fig. 3.1 depicts this process.

Then, it was deposited 100 µL per well of an Ab-QD probe diluted in ([QD]=0.33, 0.66, 1.33, 4 and 8 nM) and the plate was read on the Cytation 5. The competitive assay was carried out durring one hour with 425cpm in orbital agitation reading absorbance and fluorescence. The extitation wavelenth used was 360nm and the emission waveleth readed was 665nm. The associated results are shown in chapter IV.

From the results obtained in this assay, other concentration a few higer and lower were examined to determine the best option.

Optimization of GO concentration (procedure)

According with the working range of GO as quencher reported in previous experiments by Ortiz Riaño, the optimum concentration is in a range from 1000 µg mL^{-1} to 1600 µg mL^{-1}. [63] It was chosen a proposed concentration in this range (1200 µg mL^{-1}). And after analyzed the behavior of the platform with this concentration, it was decided to try higher and lower concentrations (form 1100 µg mL^{-1} to 1400 µg mL^{-1}) to be assure that the concentration chosen is the best option for this specific application.

Analytical characterization

The data obtained through Gen5™ needs to be analyzed to assess the success of the perform immunoassay. The analysis begins with the standardization of the data. Gen5™ gives the fluorescence intensity read in relative units of fluorescence. Using the Equation III.II in every measure made, we obtain a ratio of fluorescence intensity in every point regarding the initial intensity.

Calibration curve (or standard curve) can be used to perform interpolations and determine the analyte concentration of a sample from given its response.[64] It is acquired by logarithmic transformation of the concentrations data and a linear regression. Linear regression is the curve that better fits regarding the curves obtained from the experimental data. Calibration curve gives important information to determine the effectivity of the operating principle in which this biosensing platform is based, the main data to be obtained are listed below:

1. Limit of Detection (LOD) is the lowest concentration of the analyte that can be detected in a reliable way.[65] LOD gives information about the response of the biosensing system and it is calculated by interpolating the mean value determined by the blank plus 3 times its standard deviation into the calibration curve.

$$LOD = \bar{X} + 3\sigma \, . \qquad (Eq.\ III.I)$$

2. Slope: is a number known as gradient of a line that describe how the line is increasing or decreasing of it.[64]
3. Correlation coefficient (R^2): this parameter gives information about the fitting regarding curve fitting model. R^2 is a proportion of the variance of the independent variable that is predictable from the independent variables. [64]

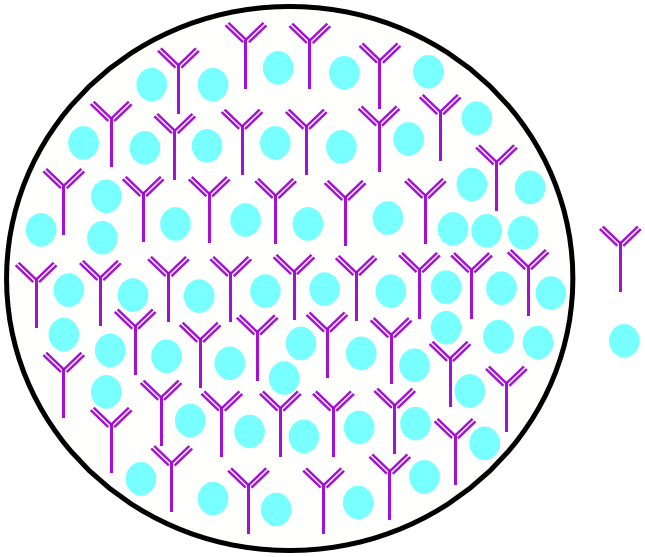

Figure 3.1. Well to conjugation anti-E. coli-quantum dots blocked with casein.

In order to operate the studied immunosensing strategy, first of all, the wells of the microwell plate are filled in with the GO suspension (with a concentration between 1100 and 1400 µg mL^{-1}). The plate is shaken overnight, and is then washed three times with Milli-Q water (ultrapure water). Then, the sample and the probe (Ab-QD), with a concentration determined by the optimization explained above, is deposited in a well. The sample concentrations used in the immunosensing platform accounts from zero to 10^6 CFU mL^{-1}. Three parallel experiments were performed by using 3 microwell (for statistics), and all the experiments include a blank sample (three wells), which is a control of the fluorescence quenching in the absence of bacteria. Finally, the plate is placed in the Cytation 5 to carry out the respective analysis. The first step in the analysis is the fluorescence intensity determination, initial intensity (I_0). Immediately it will begin the kinetic measurement, making a measurement every 5 minutes by 2 hours. In every measure it is determinate a final intensity (I_f). Quenching fluorescence is defined with these parameters as:

$$quenching = \frac{Final\ Intensity}{Initial\ Intensity} = \frac{I_f}{I_o}. \qquad (Eq.\ III.II)$$

Selectivity test

As explained above, selectivity is one of the most important characteristics of a biosensor, given this characteristic a biosensing system exhibits the capability to selectively distinguish between the target analyte and other species that could be present in the analyzed sample. [18,66,67]

In order to prove that cross reactivity is not occurring in the resulting biosensing system, it was used a sample of *Salmonella typhimurium* strain as a non-target pathogen. The following samples were chosen to demonstrate the selectivity of the studied biosensing system:

a) Serial dilutions of *Salmonella* from 5 to 10^6CFU mL^{-1}, in PBS.
b) A mixture of a high concentration of *E. coli* (10^5 CFU mL^{-1}) with a high concentration of *Salmonella* (10^5 CFU mL^{-1}).
c) A mixture of a low concentration of *E. coli* (10^3 CFU mL^{-1}) with a high concentration of *Salmonella* (10^5 CFU mL^{-1}).

The biosensing system was assayed with theses samples following the afore mentioned general procedure; that is to say, by adding the samples in the corresponding microwell previously coated with GO, and adding the probe to perform the kinetic analysis in the microplate reader during 120 minutes.

Real Sample Test

"La Próxima Estación" is a company that allowed the link between this investigation project and the industry. "La Próxima Estación" provided us with real samples of frozen food. These samples are prepared in PBS by adding 10% of the vegetable selected (w/v). For this preparation, 10 grams are weighed, finely chopped and added to 90 mL of PBS. Then, they put the mixture in a sterile plastic bag and it is homogenized by a Stomacher. A Stomacher is a mixing device suitable for preparing bacterial suspensions from food, the sterile plastic bag is vigorously pounded on its outer surfaces by paddles when placed inside the machine. The resulting compression and shearing forces effectively detach even deep-seated bacteria.[68] The vegetables tried were cauliflower and spinach. The principal difference among ideal and real sample is the matrix behind of the food samples that is more complex and less transparent.

Chapter 4. RESULTS

This chapter includes the results given by the experiments explained in chapter 3. The best results for bionanoreagents optimization were chosen based on the analytical characterization. The selectivity test was accepted as successful by comparison with the assay made with the model analyte. For the real sample test, it was needed an extra analysis that is explained and presented in the real sample section. In this chapter are presented only the results of the experiments with the best performance and the Appendix includes general experiments supporting these optimized results, thus offering a general idea about the evolution of the project.

Bionanoreagents optimization

To provide the optimal conditions with the best efficiency, the Ab concentration was kept constant (100µg mL^{-1}) and different QDs concentrations were examined (8, 4, 1.33, 0.66 and 0.33nM) in a competitive assay during one hour. Fig. 4.1 is a graph obtained from the assay, which shows the fluorescence emitted by the explored QDs concentrations measured in Relative Fluorescence Units (RFU). With [QD]=0.33nM the fluorescence exhibited is practically zero whereby it is not of interest to this project. However, concentration of 8nM exhibit more relative fluorescence units, which give the possibility of reporting a bigger amount of conjugated Ab. According to this result is estimated that the optimal concentration of conjugation of QDs may be find at 8nM or in a bigger concentration.

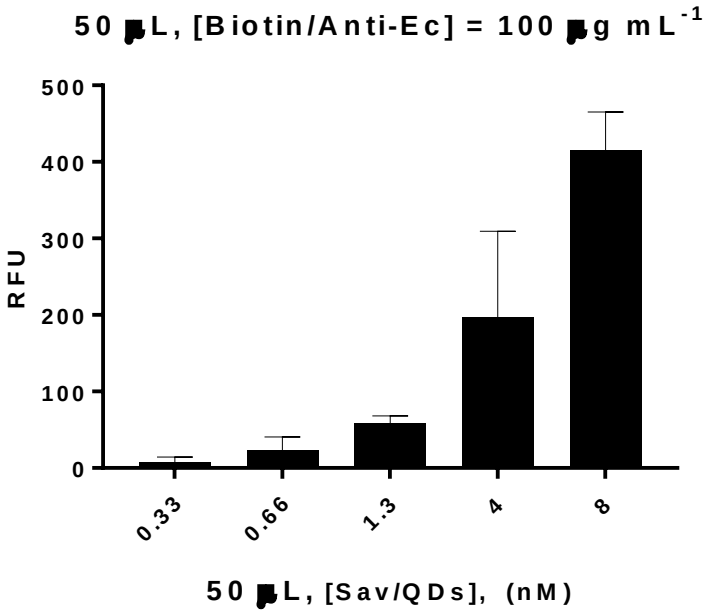

Figure 4.1 Competitive assay Anti-E. coli VS QDs for conjugation optimization

The first test was done during 215 minutes to define the duration and the volume of the test. The probe used was [Ab]=25µg mL^{-1} + [QDs]=0.1nM on [GO]=1200µg mL^{-1} coating. With 50µL of probe and 50µL of sample. Samples used was of *E. coli* (strain diluted in PBS) in concentrations from 5 to 10^6 CFU mL^{-1}. In Fig. 4.2 is shown the kinetics of the experiment, where the y axis represents the fluorescence quenching and the x axis represents the time. Based on this result, the time of the test was reduced to 120 minutes and the volume of the sample and the probe were increased to 100µL each in coming assays.

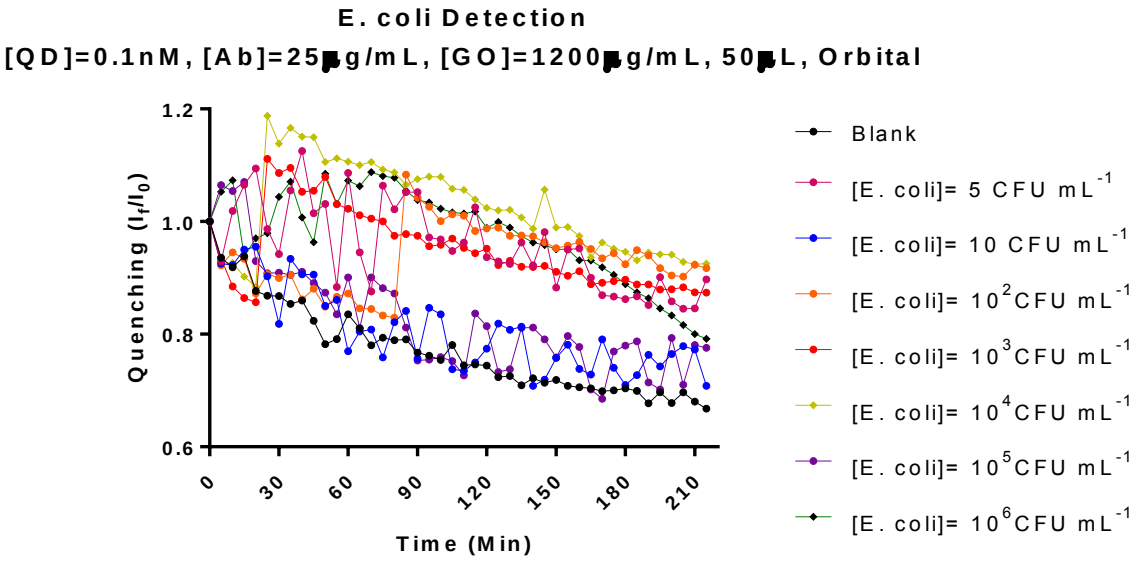

Figure 4.2. E. coli detection during 215 minutes, first approximation

[GO]= 1200µg mL^{-1} was chosen according with the working range of GO as quencher reported in previous experiments by Ortiz Riaño.[63] To be assure that [GO]=1200µg mL^{-1} gives the best performance as quencher for this application, it was examined higher and lower concentration of GO. In Fig. 4.3 is shown the kinetics answer obtained with [GO]=1100, 1200, 1300 and 1400 µg mL^{-1} respectively. Despite [GO]=1200µg mL^{-1} and [GO]=1400µg mL^{-1} exhibit a similar quencher behavior, the detection is better in 1200 µg mL^{-1} than in 1400 µg mL^{-1}, because in 1200 µg mL^{-1} the difference between one concentration and another is pronounced. In other words, with [GO]=1200µg mL^{-1} exist a bigger separation between the kinetics lines. These assays confirm that [GO]=1200µg mL^{-1} is the optimum concentration for this application.

Also, it was tried some other different concentrations of QDs. The best results obtained was with: [Ab]=72µg mL^{-1} + [QDs]=9nM conjugated and diluted up to [Ab]=0.9µg mL^{-1} + [QDs]=0.1125nM. These conditions were tried in samples of *E. coli* in concentrations from 5 to 10^6 CFU mL^{-1}. In Fig. 4.4 is observed the kinetics answer of the system, and in Fig. 4.5 a bar chart that allows to compare the quenching provoked by a sample in different moments of the assay. The ratio of quench fluorescence reach in these conditions for the blank sample at 120 minutes was 0.43, and for the most concentrated sample of *E. coli* was 0.57. Notably, the behavior in bar chart is the expected; the more *E. coli* concentration, the less quenching fluorescence. Also, should be mentioned that the error bars of the blank sample at 30 minutes are almost imperceptible, that could mean that 30 minutes is the optimum time for the measurement. Although Fig. 4.4 and 4.5 present the optimum conditions found,

many more experiments were realized before find and chose these parameters, some of these experiments results are shown in Section 1. of the Appendix I.

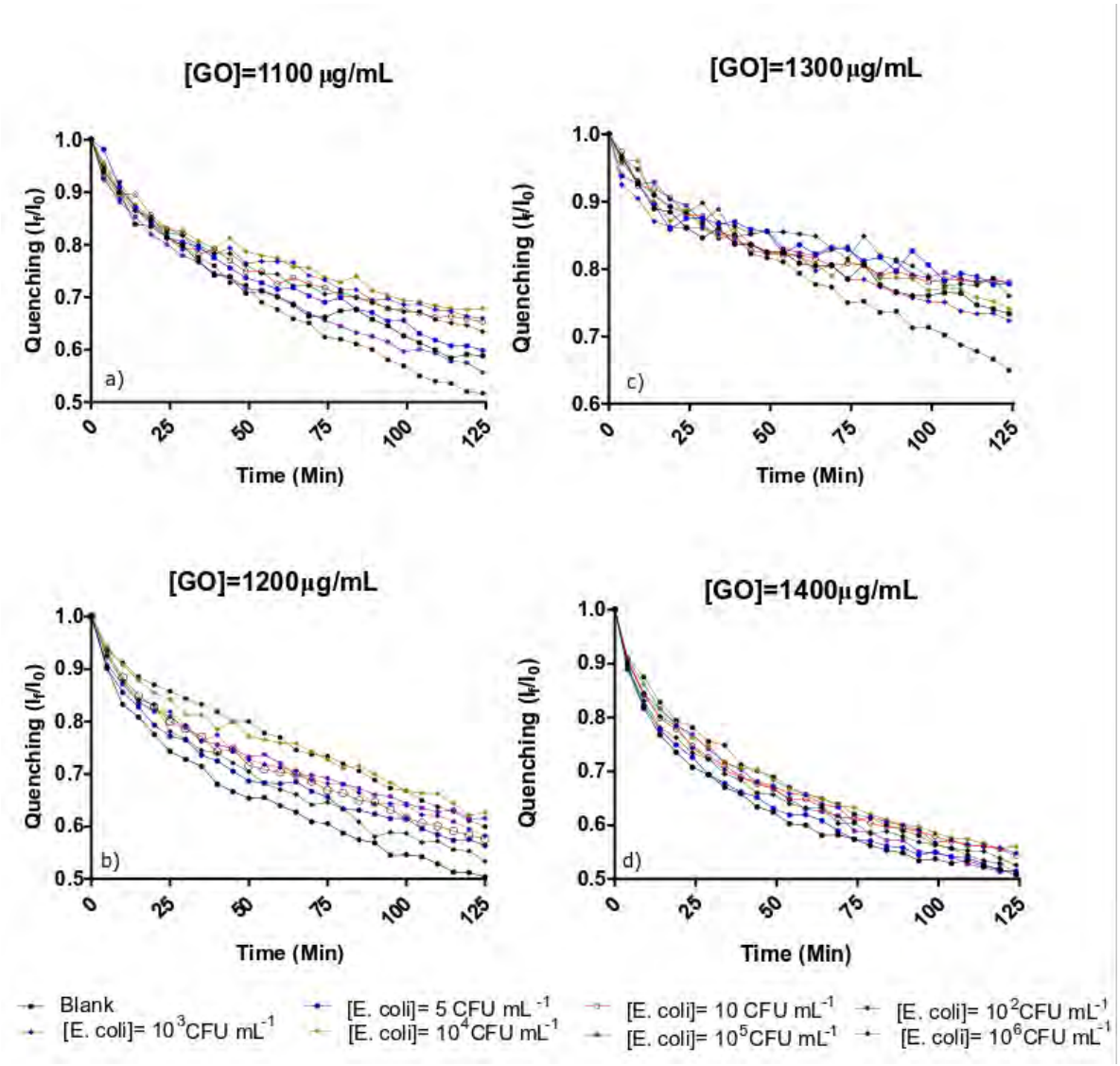

Figure 4.3. Behavior of the biosensing platform with different concentrations of GO. E. coli detection, [QD]=0.1nM, [Ab]=1.25µg mL^{-1}, 100µL, orbital agitation. a) [GO]=1100 µg mL^{-1}. b)1300 µg mL^{-1}. c) 1200 µg mL^{-1}. d) 1400 µg mL^{-1}.

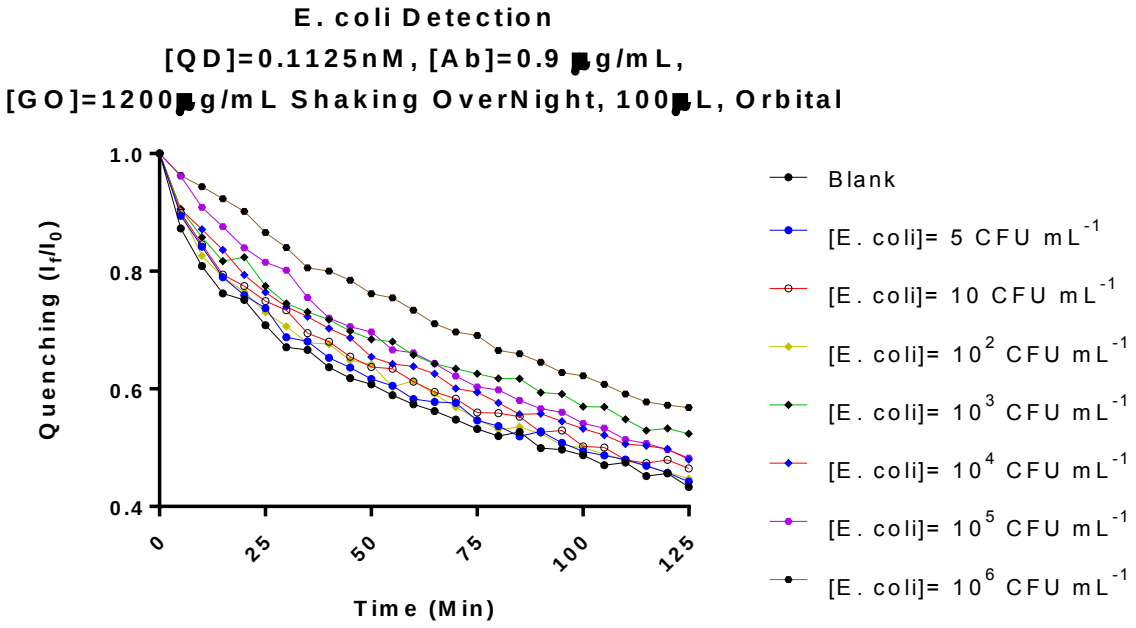

Figure 4.4. E. coli kinetic detection in optimum conditions

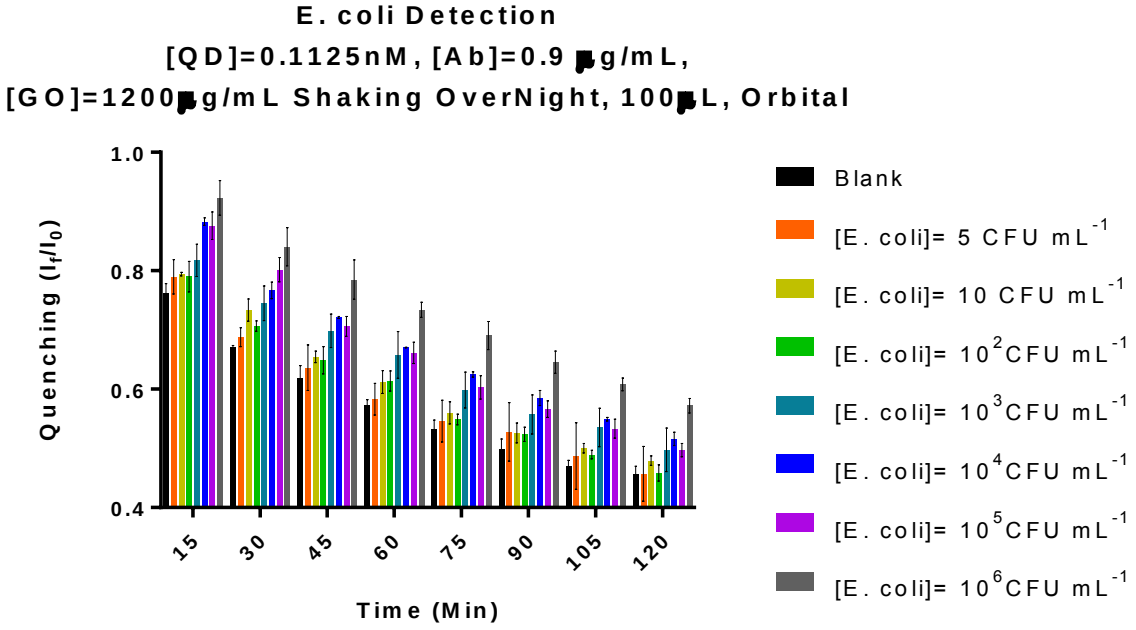

Figure 4.5. Bar chart of E. coli detection

Analytical characterization

For the analytical characterization of the data obtained, it was necessary to make a logarithmic transformation of the concentration sample data and then a linear regression. Fig. 4.6 shows the calibration curves obtained with the linear regression. Also, Table 4.1 summarizes the validation parameters obtained in several experiments made with different conditions. Based on this analysis is was selected the calibration curve shown in Fig. 4.6 as the best option at 30 minutes. The LOD of 1.8 CFU mL^{-1} and R^2=0.8686, mainly represent the parameters which assure that the optimum reagent concentrations are [QD]=11.25nM, [Ab]=0.9 µg mL^{-1} and [GO]=1200µg mL^{-1}, with a volume of sample and probe of 100µL each and the optimum time of detection at 30 minutes. Table 4.1 shows the maximum and the minimum of coefficient variation of every parameter mentioned. For more information, in Section 2. of Appendix I are listed the coefficient variation for every concentration of *E. coli* sample examined.

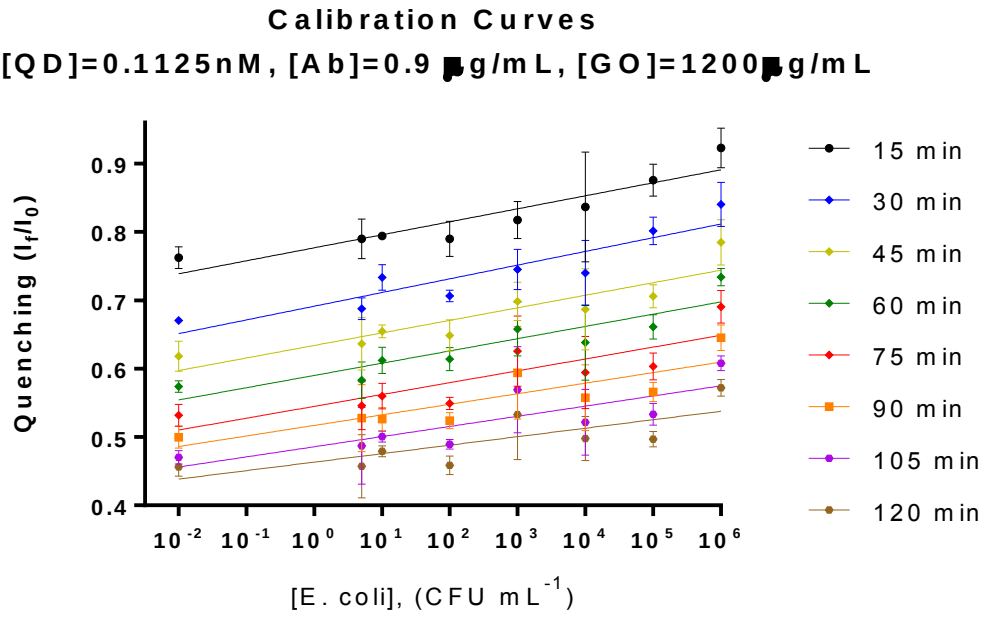

Figure 4.6. Calibration curve with the conditions chosen as optimum

It should be remembered that all of this behavior is reached in the ideal case, using as sample a laboratory strain *E. coli*. This analysis allows to choose the optimum conditions of the biosensing platform, but below will be discussed the behavior of the system with real samples.

Table 4. Comparison of parameters of different experiments and conditions. All the experiments used [GO]=1200µg mL^{-1}.

Date aammdd	**QD (nM)**	**Ab (µg mL^{-1})**	**Time (Min)**	**R^2**	**1/slope**	**LOD (CFU mL^{-1})**	**CV (SD/m) *100**
181017	0.1125	0.9	15	0.9214	42.37	143.21	0.38-9.63%
181017	***0.1125***	***0.9***	***30***	***0.8686***	***40.74***	***1.81***	***0.49-6.42%***
181003	0.1125	1.25	15	0.9343	40.76	16557.69	1.18-5-70%
181003	0.1125	1.25	30	0.8385	35.56	210.37	0.26-8.76%
181017	0.1125	1.5	15	0.9596	34.68	8.22	0.43-3.97%
181017	0.1125	1.5	30	0.93	36.44	14.28	0.76-3.17%

Inter-assay coefficient of variation

To define the inter-assay precision, it was calculated de coefficient of variation (CV) of 3 different assays realized in the optimal conditions. The CV minimum and maximum are shown in Table 5. For blank sample, comparing the 3 assays results, there is a CV from 3.41 to 5.61%. Whereas, the variation for *E. coli* sample concentrations (5-10^6 CFU mL^{-1}) is from 2.99 to 5.67%. According with the Food and Drug Administration (FDA) guidelines the acceptance criteria for these types of procedures are less than 30% of CV.[69,70] Following these guidelines this proposed platform is far below this limit, considering in this way very precise. Besides, Section 3 of Appendix I includes the CV calculated at every time considered throughout the assay. Also, in Fig. 4.7 can be observed a mean of the results obtain for blank and *E. coli* sample in 3 different assays under the same conditions in a bar chart.

Table 5. Inter-assay coefficient of variation (max. and min. by sample)

Date	CV of blank sample	CV of [E. coli] =10^3 CFU mL^{-1} sample
181017 190312 190311	3.41-5.61 %	2.99-5.67 %

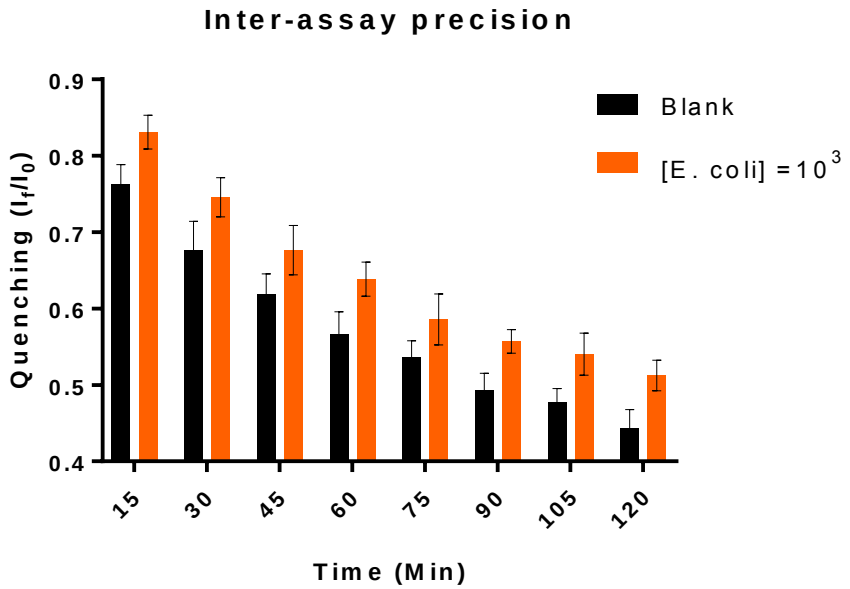

Figure 4.7. Inter-assay precision. Mean of the blank and E. coli samples of 3 different assays. The sample of E. coli is measured in CFU mL^{-1}

In summary, according with the information shown if Figures 4.4, 4.5 and 4.6 the optimum conditions were found with [GO]=1200 µg mL^{-1}, [Ab]=0.9 µg mL^{-1} and [QD]=0.9nM, reaching a LOD of 1.8 CFU mL^{-1}. Besides with these conditions the time of response is around 45 minutes that is too much faster that the culture-based test. Also, in comparison with the background of biosensing platforms presented in chapter 1 the proposed optical biosensing platform exhibit a lower LOD giving it an advantage over the others mentioned before. Besides the inter-assay precision analysis, demonstrates the reliability of the test.

Selectivity test

With the results obtained in the reagent optimization, the assay was replicated but the sample was a *Salmonella* strain. For *Salmonella* in concentrations from zero to 10^6 the results obtained are shown in Fig. 4.8 a), in comparison with the *E. coli* strain assay is evident the difference in the behavior. In fact, all the *Salmonella* samples exhibit a quenching similar to the blank. Also, in the bar chart presented in Fig. 4.8 b) is easier to see that all the bars reach the same height which means that all the samples experiment the same fluorescence quenching.

Other assay that proof the high selectivity of the biosensing platform was using a mixture of a high concentration of *E. coli* (10^5 CFU mL^{-1}) with a high concentration of *Salmonella* (10^5 CFU mL^{-1}) as sample. Compared with a mixture of a low concentration of *E. coli* (10^3 CFU mL^{-1}) with a high concentration of *Salmonella* (10^5 CFU mL^{-1}) and a blank sample. The kinetics of the assay is presented in Fig. 4.8 c) where is shown that in presence of *E. coli* the probe keeps its fluorescence and there is an apparent difference between the mixture samples and the blank despite the presence of *Salmonella*, which does not interfere in the detection. Besides, in Fig. 4.8 d) the bar chart shows that in every moment of the assay the difference between the blank and the mixed sample is perceived at a glance.

All these assays demonstrate the selectivity of the antibody used and allows to proceed to try with real samples, assuring that there is not cross reactivity.

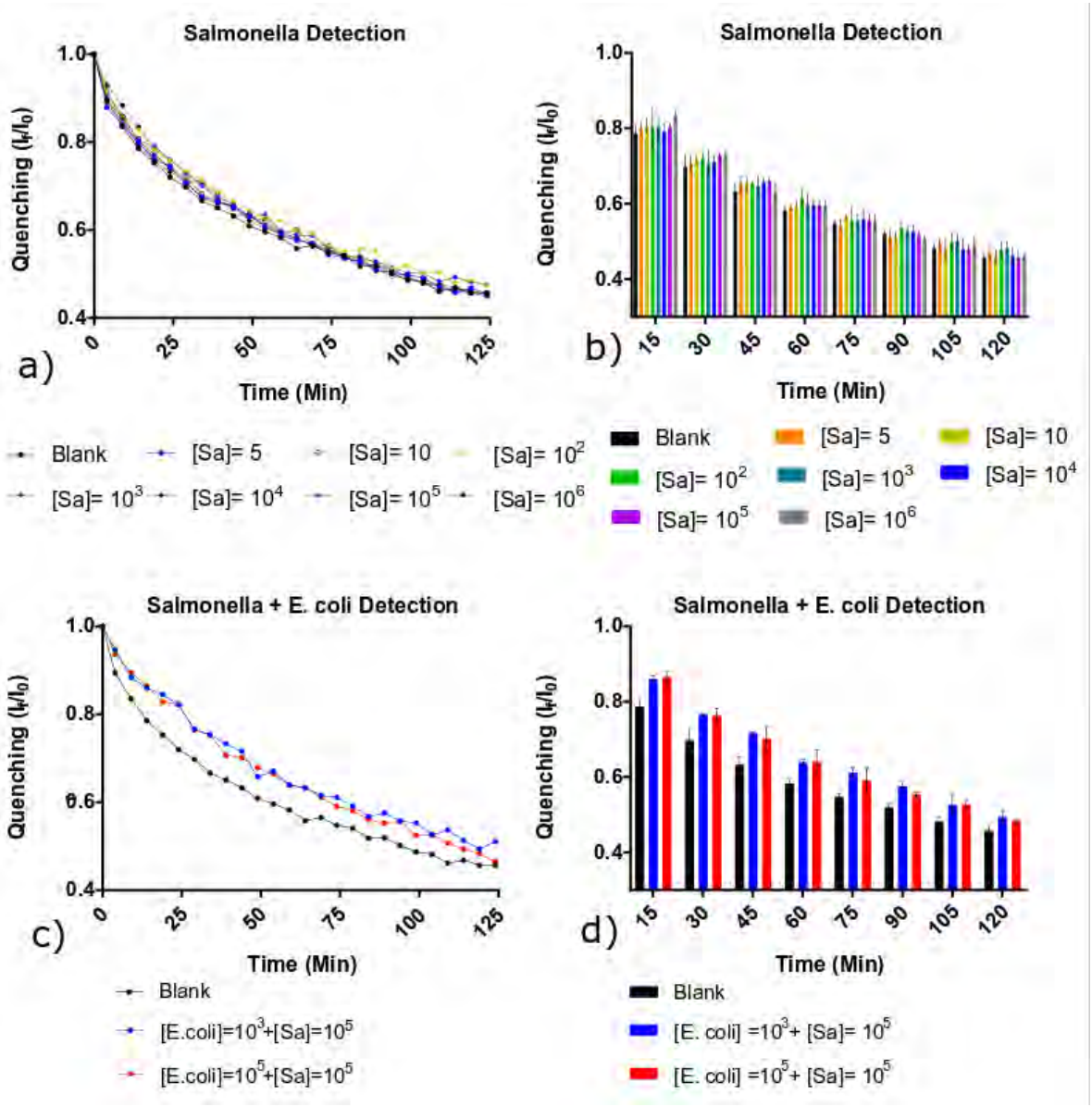

Figure 4.8. Selectivity test in conditions: [GO]=1200 µg mL^{-1}, [QD]=0.1125nM, [Ab]=0.9 µg mL^{-1}. a) Kinetics with Salmonella samples. b) Bar chart Salmonella samples. c) Kinetics E. coli + Salmonella samples. d) Bar chart E. coli + Salmonella Samples. (All the concentration samples are measured in CFU mL^{-1}).

Real Sample Test

As real samples were used vegetables such as spinach and cauliflower. The samples were prepared as described in experimental methodology section. The sample analyzed by the proposed biosensing platform also were analyzed by the company in its laboratory by the method of cultured-based assay (a gold standard method) that is described in the first chapter. In this manner, we can compare the results obtained by the two methods. Under the idea of the sample may have a high concentration which could provoke a saturation of the sensor and also because of the complex matrix given by the

vegetables, the samples were diluted in PBS. Several dilutions were tried to analyze the received response and determine the best dilution for each kind of sample.

Cauliflower samples were tried in dilutions from 1 to 1/400 (v/v), to demonstrate the hypothesis that the sample delivered by the company requires another dilution for the good performance of the sensing. The results obtained for all these dilutions are shown in Section 4 of Appendix I. Cauliflower were analyzed in two presentations chopped cauliflower and mashed cauliflower, for both was observed the same behavior. Fig. 4.9 is the kinetic analysis of the samples with a dilution of 1/4 and Fi. 4.10 shows the bar chart of the assay; The response is not clear to the eye and there is many information. To better visualize the behavior of the assay, it was decided to make a normalization regarding to the blank. Then it was observed that at 45 minutes the response is the clearer. This normalization is shown in Fig. 4.11 where, vertical axis represents the quenching normalization and the horizontal axis shows the sample used, the pointed line is for visualized easily the difference between positive and negative samples. Showing the normalization regarding to the blank is clearer the difference between the samples reported as negatives by the company (N1, N2, N3, N4) of *E. coli* contamination and the other reported as positives of *E. coli* contamination (P1, P2, P3, P4). In comparison with the data given by the company the assay exhibits a 100% of effectivity and also 100% of sensibility.

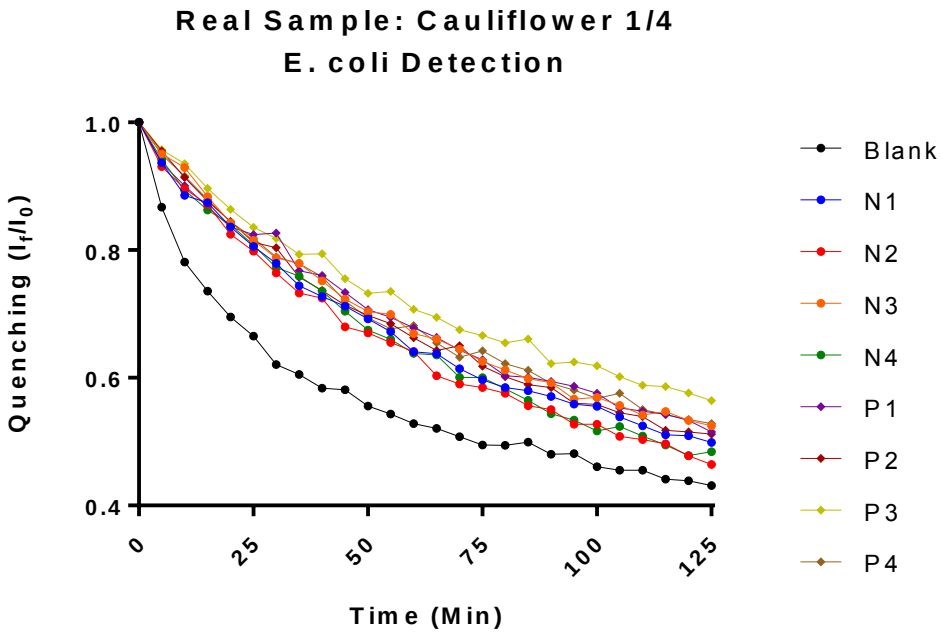

Figure 4.9. Kinetic E. coli detection in Real sample (Cauliflower 1/4)

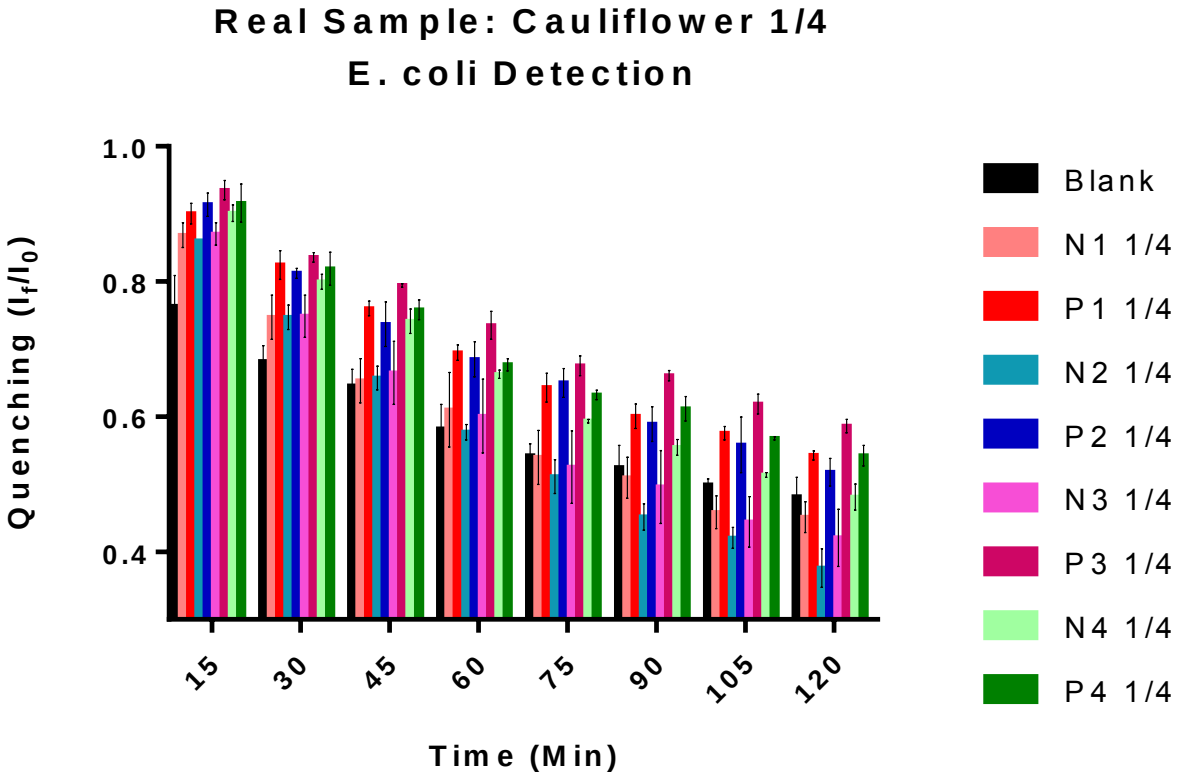

Figure 4.10. Bar chart E. coli detection in Real sample (Cauliflower 1/4)

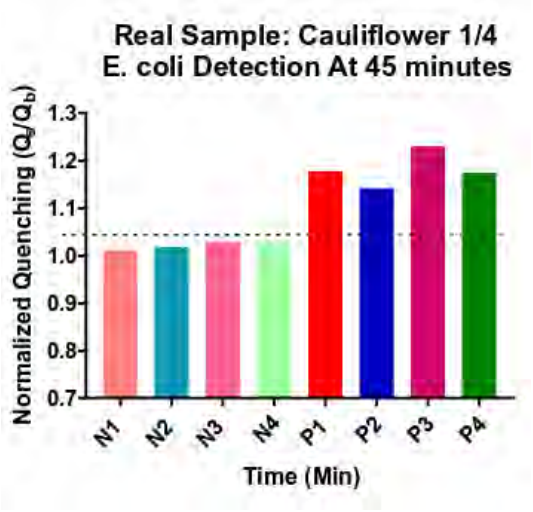

Figure 4.11. Normalization regarding to the blank. E. coli detection in real sample (cauliflower 1/4) at 45 min.

Spinach samples were used in dilutions from 1/4 to 1/80 (v/v) and the best response were obtained in a dilution of 1/20 (v/v). Section 4 of Appendix I. shows the results obtained for all these dilutions. Fig. 4. 12 is the kinetic response obtained from this assay, making a comparative of the kinetic

behavior of all the samples studied. Fig. 4.13 illustrate the results obtained in the assay, also presenting the normalization regarding to the blank. The company informed that the samples 408, 329, 3664, and 073 results positives of *E. coli* contamination whereas for this assay samples 408, 364, 336 and 073 results as positives of *E. coli* contamination but, sample 329 may be a false negative. Besides, samples 300, 333, 340, 373 and 403 are negatives of *E. coli* contamination regarding with the company while, in this test samples 300, 333, 340, 373 results negative of *E. coli* contamination but sample 403 results as a false positive. From this assay and comparing the results obtained with the results informed by the company the proposed biosensing platform exhibit an 80% of effectivity and an 80% of sensibility.

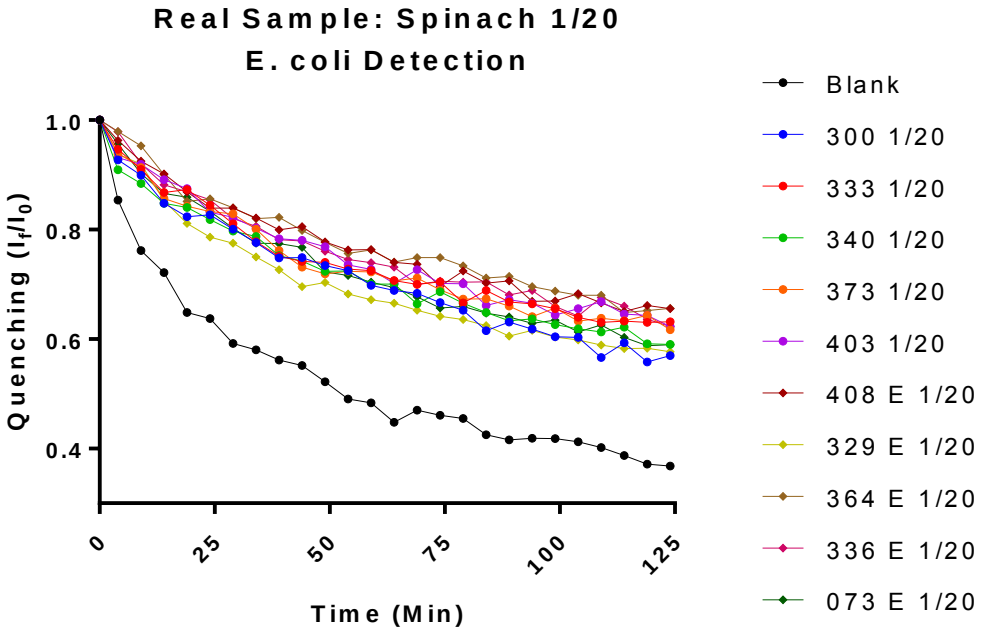

Figure 4.12. Kinetic E. coli detection in Real sample (Spinach 1/20)

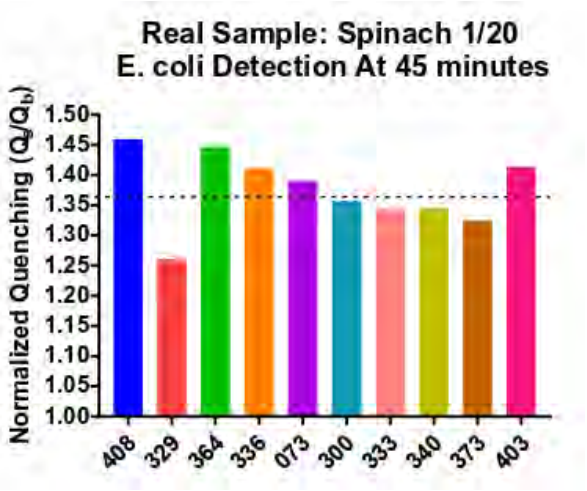

Figure 4.13. Normalization regarding to the blank. E. coli detection in real sample (Spinach 1/20) at 45 minutes.

Chapter 5. CONCLUSIONS

Taking advantage of the quenching capabilities of GO, it was developed a novel, cost-effective, quick response biosensing platform able to determine pathogenic bacteria contamination in food industry samples. The biosensing platform developed can be described as a one-step immunoassay; once the microwell plate are prepared with graphene oxide, the detection only requires: a mix of the sample with the probe and read and interpreted the signal. It was demonstrated that the operational principle based on FRET phenomena between GO, as acceptor, and QD as donor works correctly for this application. Also, it was found the optimum concentration for each reagent ([GO]=1200µg mL^{-1}, [Ab]=0.9µg mL^{-1} and [QD]=0.1125nM), reaching a LOD of up to 1.8 CFU mL^{-1} and a time response of around 30 minutes. This biosensing platform works for *E. coli* strain samples from zero to 10^6 CFU mL^{-1}, out of this range the platform can become saturated. In the described conditions, it was proved that cross reactivity is not occurring through assays with different samples of *Salmonella* strain. In addition, the immunosensing platform was tested with industrial food samples, due to the complex matrix presented by the analyzed vegetables samples the response obtained allows to determine in a qualitative way if the tested sample is contaminated or not. To get these results it was necessary to dilute the sample supplied by the company. Also, it was necessary to make a second analysis of the results obtained. For cauliflower the dilution required was 1/4 (v/v) with a time response of 45 minutes, comparing the results with the information given by the company, the assay reach 100% of effectivity and 100% of sensibility. Regarding spinach samples results the dilution required was 1/20 (v/v) with a time response of 45 minutes; reaching 80% of effectivity and 80% of sensibility. About the cost reduction, the estimated cost per test is $8.08 MXN, ergo $2.69 MXN per well. In contrast of the culture- based assay that have an estimated cost of $65.00 MXN per test using 3M™ Petrifilm™ *E. coli* / Coliform Count (EC) Plate. Because of the proposed biosensing platform is considerate as an immunoassay, it is important to compare it with an ELISA, the gold immunoassay; Which in a commercial kit offer a LOD of around $4x10^5$ CFU mL^{-1} and cost $95 per test. Appendix I, Section 5 details the cost estimation of the proposed biosensing platform and a comparision table with the cuture- base method and ELISA immunoassay. All in all, it was developed a sensitive, selective, inexpensive, quick responsive, optical biosensing platform which allows for the determination of *E. coli* in food contamination in vegetables such as cauliflower and spinach, for agro-food industry. Hence, potentially offering “La Próxima Estación” a faster and cheaper option to assure the quality of the product and the consumer safety.

FUTURE WORK

As part of the future work proposed is to increase *n*, for validation with a bigger number of samples. In this manner the platform may be consolidated as a potential alternative not only for "La Próxima Estación", but for every food industry company. Moreover, transfer the technology of the proposed biosensing platform to a lateral flow platform would give to "La Próxima Estación" a ready to use dispositive, that is whys transfer this technology is also considerate as future work. Finally, other point proposed as part of the future perspectives of this work is to transfer the technology to others analytes, for example, for cell cancer detection.

REFERENCES

(1) Luo, K.; Kim, H.-Y.; Oh, M.-H.; Kim, Y.-R. Paper-Based Lateral Flow Strip Assay for the Detection of Foodborne Pathogens: Principles, Applications, Technological Challenges and Opportunities. *Crit. Rev. Food Sci. Nutr.* **2018**, 1–14. https://doi.org/10.1080/10408398.2018.1516623.

(2) CDC. Prevent Shiga Toxin-Producing E. coli Infection https://www.cdc.gov/ecoli/ecoli-prevention.html (accessed May 28, 2019).

(3) E. coli https://www.who.int/news-room/fact-sheets/detail/e-coli (accessed May 28, 2019).

(4) E. Coli Outbreaks Fast Facts - CNN https://edition.cnn.com/2013/06/28/health/e-coli-outbreaks-fast-facts/index.html (accessed May 28, 2019).

(5) Wang, Y.; Duncan, T. V. Nanoscale Sensors for Assuring the Safety of Food Products. *Food Biotechnol. • Plant Biotechnol.* **2017**, *44*, 74–86. https://doi.org/10.1016/j.copbio.2016.10.005.

(6) Srivastava, A. K.; Dev, A.; Karmakar, S. Nanosensors and Nanobiosensors in Food and Agriculture. *Environ. Chem. Lett.* **2018**, *16* (1), 161–182. https://doi.org/10.1007/s10311-017-0674-7.

(7) Majdinasab, M.; Hayat, A.; Marty, J. L. Aptamer-Based Assays and Aptasensors for Detection of Pathogenic Bacteria in Food Samples. *TrAC Trends Anal. Chem.* **2018**, *107*, 60–77. https://doi.org/10.1016/j.trac.2018.07.016.

(8) Wu, S.-Y.; Hulme, J.; An, S. S. A. Recent Trends in the Detection of Pathogenic Escherichia Coli O157 : H7. *BioChip J.* **2015**, *9* (3), 173–181. https://doi.org/10.1007/s13206-015-9208-9.

(9) Chen, J.; Andler, S. M.; Goddard, J. M.; Nugen, S. R.; Rotello, V. M. Integrating Recognition Elements with Nanomaterials for Bacteria Sensing. *Chem. Soc. Rev.* **2017**, *46* (5), 1272–1283. https://doi.org/10.1039/C6CS00313C.

(10) Austin, J. W.; Pagotto, F. J. MICROBIOLOGY | Detection of Foodborne Pathogens and Their Toxins. In *Encyclopedia of Food Sciences and Nutrition (Second Edition)*; Caballero, B., Ed.; Academic Press: Oxford, 2003; pp 3886–3892. https://doi.org/10.1016/B0-12-227055-X/00774-4.

(11) Lequin, R. M. Enzyme Immunoassay (EIA)/Enzyme-Linked Immunosorbent Assay (ELISA). *Clin. Chem.* **2005**, *51* (12), 2415. https://doi.org/10.1373/clinchem.2005.051532.

(12) van Weemen, B. K. The Rise of EIA/ELISA. *Clin. Chem.* **2005**, *51* (12), 2226. https://doi.org/10.1373/clinchem.2005.059626.

(13) Duan, Y. F.; Ning, Y.; Song, Y.; Deng, L. Fluorescent Aptasensor for the Determination of Salmonella Typhimurium Based on a Graphene Oxide Platform. *Microchim. Acta* **2014**, *181* (5), 647–653. https://doi.org/10.1007/s00604-014-1170-4.

(14) Morales-Narváez, E.; Naghdi, T.; Zor, E.; Merkoçi, A. Photoluminescent Lateral-Flow Immunoassay Revealed by Graphene Oxide: Highly Sensitive Paper-Based Pathogen Detection. *Anal. Chem.* **2015**, *87* (16), 8573–8577. https://doi.org/10.1021/acs.analchem.5b02383.

(15) Morales-Narváez, E.; Hassan, A.-R.; Merkoçi, A. Graphene Oxide as a Pathogen-Revealing Agent: Sensing with a Digital-Like Response. *Angew. Chem. Int. Ed.* **2013**, *52* (51), 13779–13783. https://doi.org/10.1002/anie.201307740.

(16) Zuo, P.; Li, X.; Dominguez, D. C.; Ye, B.-C. A PDMS/Paper/Glass Hybrid Microfluidic Biochip Integrated with Aptamer-Functionalized Graphene Oxide Nano-Biosensors for One-Step

Multiplexed Pathogen Detection. *Lab. Chip* **2013**, *13* (19), 3921–3928. https://doi.org/10.1039/C3LC50654A.
(17) Cheeveewattanagul, N.; Morales-Narváez, E.; Hassan, A.-R. H. A.; Bergua, J. F.; Surareungchai, W.; Somasundrum, M.; Merkoçi, A. Straightforward Immunosensing Platform Based on Graphene Oxide-Decorated Nanopaper: A Highly Sensitive and Fast Biosensing Approach. *Adv. Funct. Mater.* **2017**, *27* (38), 1702741. https://doi.org/10.1002/adfm.201702741.
(18) Chakraborty, M.; Hashmi, M. S. J. An Overview of Biosensors and Devices. In *Reference Module in Materials Science and Materials Engineering*; Elsevier, 2017. https://doi.org/10.1016/B978-0-12-803581-8.10316-9.
(19) Zuber, A. A.; Klantsataya, E.; Bachhuka, A. 3.06 - Biosensing. In *Comprehensive Nanoscience and Nanotechnology (Second Edition)*; Andrews, D. L., Lipson, R. H., Nann, T., Eds.; Academic Press: Oxford, 2019; pp 105–126. https://doi.org/10.1016/B978-0-12-803581-8.10410-2.
(20) Chapter 9 - Antibodies. In *Immunology for Pharmacy*; Flaherty, D. K., Ed.; Mosby: Saint Louis, 2012; pp 70–78. https://doi.org/10.1016/B978-0-323-06947-2.10009-4.
(21) Otieno, B. A.; Krause, C. E.; Rusling, J. F. Chapter Seven - Bioconjugation of Antibodies and Enzyme Labels onto Magnetic Beads. In *Methods in Enzymology*; Kumar, C. V., Ed.; Academic Press, 2016; Vol. 571, pp 135–150. https://doi.org/10.1016/bs.mie.2015.10.005.
(22) Godbey, W. T. Chapter 8 - Fluorescence. In *An Introduction to Biotechnology*; Godbey, W. T., Ed.; Woodhead Publishing, 2014; pp 173–186. https://doi.org/10.1016/B978-1-907568-28-2.00008-3.
(23) Wouterlood, F. G.; Boekel, A. J. Fluorescence Microscopy in the Neurosciences. In *Encyclopedia of Neuroscience*; Squire, L. R., Ed.; Academic Press: Oxford, 2009; pp 253–260. https://doi.org/10.1016/B978-008045046-9.00666-5.
(24) Strianese, M.; Staiano, M.; Ruggiero, G.; Labella, T.; Pellecchia, C.; D'Auria, S. Fluorescence-Based Biosensors. In *Spectroscopic Methods of Analysis: Methods and Protocols*; Bujalowski, W. M., Ed.; Humana Press: Totowa, NJ, 2012; pp 193–216. https://doi.org/10.1007/978-1-61779-806-1_9.
(25) Morales-Narváez, E.; Pérez-López, B.; Pires, L. B.; Merkoçi, A. Simple Förster Resonance Energy Transfer Evidence for the Ultrahigh Quantum Dot Quenching Efficiency by Graphene Oxide Compared to Other Carbon Structures. *Carbon* **2012**, *50* (8), 2987–2993. https://doi.org/10.1016/j.carbon.2012.02.081.
(26) Clegg, R. M. Chapter 1 Förster Resonance Energy Transfer—FRET What Is It, Why Do It, and How It's Done. In *Laboratory Techniques in Biochemistry and Molecular Biology*; Elsevier, 2009; Vol. 33, pp 1–57. https://doi.org/10.1016/S0075-7535(08)00001-6.
(27) Melle, S.; Calderón, O. G.; Laurenti, M.; Mendez-Gonzalez, D.; Egatz-Gómez, A.; López-Cabarcos, E.; Cabrera-Granado, E.; Díaz, E.; Rubio-Retama, J. Förster Resonance Energy Transfer Distance Dependence from Upconverting Nanoparticles to Quantum Dots. *J. Phys. Chem. C* **2018**, *122* (32), 18751–18758. https://doi.org/10.1021/acs.jpcc.8b04908.
(28) Clapp, A. R.; Medintz, I. L.; Mattoussi, H. Förster Resonance Energy Transfer Investigations Using Quantum-Dot Fluorophores. *ChemPhysChem* **2006**, *7* (1), 47–57. https://doi.org/10.1002/cphc.200500217.
(29) Nasrollahzadeh, M.; Sajadi, S. M.; Sajjadi, M.; Issaabadi, Z. Chapter 1 - An Introduction to Nanotechnology. In *Interface Science and Technology*; Nasrollahzadeh, M., Sajadi, S. M., Sajjadi, M., Issaabadi, Z., Atarod, M., Eds.; Elsevier, 2019; Vol. 28, pp 1–27. https://doi.org/10.1016/B978-0-12-813586-0.00001-8.

(30) Zamora-Gálvez, A.; Morales-Narváez, E.; Mayorga-Martinez, C. C.; Merkoçi, A. Nanomaterials Connected to Antibodies and Molecularly Imprinted Polymers as Bio/Receptors for Bio/Sensor Applications. *Appl. Mater. Today* **2017**, *9*, 387–401. https://doi.org/10.1016/j.apmt.2017.09.006.
(31) Hu, X.; Dong, S. Metal Nanomaterials and Carbon Nanotubes—Synthesis, Functionalization and Potential Applications towards Electrochemistry. *J. Mater. Chem.* **2008**, *18* (12), 1279–1295. https://doi.org/10.1039/B713255G.
(32) Pokropivny, V. V.; Skorokhod, V. V. Classification of Nanostructures by Dimensionality and Concept of Surface Forms Engineering in Nanomaterial Science. *EMRS 2006 Symp. Curr. Trends Nanosci. - Mater. Appl.* **2007**, *27* (5), 990–993. https://doi.org/10.1016/j.msec.2006.09.023.
(33) Akbarzadeh, A.; Samiei, M.; Davaran, S. Magnetic Nanoparticles: Preparation, Physical Properties, and Applications in Biomedicine. *Nanoscale Res. Lett.* **2012**, *7* (1), 144–144. https://doi.org/10.1186/1556-276X-7-144.
(34) Sandhu, A.; Handa, H.; Abe, M. Synthesis and Applications of Magnetic Nanoparticles for Biorecognition and Point of Care Medical Diagnostics. *Nanotechnology* **2010**, *21* (44), 442001. https://doi.org/10.1088/0957-4484/21/44/442001.
(35) Yeh, Y.-C.; Creran, B.; Rotello, V. M. Gold Nanoparticles: Preparation, Properties, and Applications in Bionanotechnology. *Nanoscale* **2012**, *4* (6), 1871–1880. https://doi.org/10.1039/c1nr11188d.
(36) Schroffenegger, M.; Reimhult, E. 2.08 - Thermoresponsive Core-Shell Nanoparticles and Their Potential Applications. In *Comprehensive Nanoscience and Nanotechnology (Second Edition)*; Andrews, D. L., Lipson, R. H., Nann, T., Eds.; Academic Press: Oxford, 2019; pp 145–170. https://doi.org/10.1016/B978-0-12-803581-8.10431-X.
(37) Suri, S.; Ruan, G.; Winter, J.; Schmidt, C. E. Chapter I.2.19 - Microparticles and Nanoparticles. In *Biomaterials Science (Third Edition)*; Ratner, B. D., Hoffman, A. S., Schoen, F. J., Lemons, J. E., Eds.; Academic Press, 2013; pp 360–388. https://doi.org/10.1016/B978-0-08-087780-8.00034-6.
(38) Sapsford, K. E.; Pons, T.; Medintz, I. L.; Mattoussi, H. Biosensing with Luminescent Semiconductor Quantum Dots. *Sensors* **2006**, *6* (8), 925–953.
(39) Morales-Narváez, E.; Baptista-Pires, L.; Zamora-Gálvez, A.; Merkoçi, A. Graphene-Based Biosensors: Going Simple. *Adv. Mater.* **2017**, *29* (7), 1604905. https://doi.org/10.1002/adma.201604905.
(40) Johari, P.; Shenoy, V. B. Modulating Optical Properties of Graphene Oxide: Role of Prominent Functional Groups. *ACS Nano* **2011**, *5* (9), 7640–7647. https://doi.org/10.1021/nn202732t.
(41) Morales-Narváez, E.; Merkoçi, A. Graphene Oxide as an Optical Biosensing Platform. *Adv. Mater.* **2012**, *24* (25), 3298–3308. https://doi.org/10.1002/adma.201200373.
(42) Zhang, H.; Zhang, H.; Aldalbahi, A.; Zuo, X.; Fan, C.; Mi, X. Fluorescent Biosensors Enabled by Graphene and Graphene Oxide. *2D Mater. Biosens. Bioelectron.* **2017**, *89*, 96–106. https://doi.org/10.1016/j.bios.2016.07.030.
(43) Ray, S. C. Chapter 2 - Application and Uses of Graphene Oxide and Reduced Graphene Oxide. In *Applications of Graphene and Graphene-Oxide Based Nanomaterials*; Ray, S. C., Ed.; William Andrew Publishing: Oxford, 2015; pp 39–55. https://doi.org/10.1016/B978-0-323-37521-4.00002-9.
(44) Li, F.; Jiang, X.; Zhao, J.; Zhang, S. Graphene Oxide: A Promising Nanomaterial for Energy and Environmental Applications. *Nano Energy* **2015**, *16*, 488–515. https://doi.org/10.1016/j.nanoen.2015.07.014.

(45) Compton, O. C.; Nguyen, S. T. Graphene Oxide, Highly Reduced Graphene Oxide, and Graphene: Versatile Building Blocks for Carbon-Based Materials. *Small* **2010**, *6* (6), 711–723. https://doi.org/10.1002/smll.200901934.
(46) Morales-Narváez, E.; Merkoçi, A. Graphene Oxide as an Optical Biosensing Platform: A Progress Report. *Adv. Mater.* **2019**, *31* (6), 1805043. https://doi.org/10.1002/adma.201805043.
(47) Loh, K. P.; Bao, Q.; Eda, G.; Chhowalla, M. Graphene Oxide as a Chemically Tunable Platform for Optical Applications. *Nat. Chem.* **2010**, *2*, 1015.
(48) Swathi, R. S.; Sebastian, K. L. Long Range Resonance Energy Transfer from a Dye Molecule to Graphene Has (Distance)−4 Dependence. *J. Chem. Phys.* **2009**, *130* (8), 086101. https://doi.org/10.1063/1.3077292.
(49) Swathi, R. S.; Sebastian, K. L. Resonance Energy Transfer from a Dye Molecule to Graphene. *J. Chem. Phys.* **2008**, *129* (5), 054703. https://doi.org/10.1063/1.2956498.
(50) Avvakumova, S.; Colombo, M.; Galbiati, E.; Mazzucchelli, S.; Rotem, R.; Prosperi, D. Chapter 6 - Bioengineered Approaches for Site Orientation of Peptide-Based Ligands of Nanomaterials. In *Biomedical Applications of Functionalized Nanomaterials*; Sarmento, B., das Neves, J., Eds.; Elsevier, 2018; pp 139–169. https://doi.org/10.1016/B978-0-323-50878-0.00006-9.
(51) Härmä, H.; Soukka, T.; Lönnberg, S.; Paukkunen, J.; Tarkkinen, P.; Lövgren, T. Zeptomole Detection Sensitivity of Prostate-Specific Antigen in a Rapid Microtitre Plate Assay Using Time-Resolved Fluorescence. *Luminescence* **2000**, *15* (6), 351–355. https://doi.org/10.1002/1522-7243(200011/12)15:6<351::AID-BIO624>3.0.CO;2-3.
(52) Hermanson, G. T. Chapter 1 - Introduction to Bioconjugation. In *Bioconjugate Techniques (Third Edition)*; Hermanson, G. T., Ed.; Academic Press: Boston, 2013; pp 1–125. https://doi.org/10.1016/B978-0-12-382239-0.00001-7.
(53) Jazayeri, M. H.; Amani, H.; Pourfatollah, A. A.; Pazoki-Toroudi, H.; Sedighimoghaddam, B. Various Methods of Gold Nanoparticles (GNPs) Conjugation to Antibodies. *Sens. Bio-Sens. Res.* **2016**, *9*, 17–22. https://doi.org/10.1016/j.sbsr.2016.04.002.
(54) Weber, P.; Ohlendorf, D.; Wendoloski, J.; Salemme, F. Structural Origins of High-Affinity Biotin Binding to Streptavidin. *Science* **1989**, *243* (4887), 85. https://doi.org/10.1126/science.2911722.
(55) Estrada-Garcia, T.; Hodges, K.; Hecht, G. A.; Tarr, P. I. Chapter 8 - Escherichia Coli. In *Foodborne Infections and Intoxications (Fourth Edition)*; Morris, J. G., Potter, M. E., Eds.; Academic Press: San Diego, 2013; pp 129–164. https://doi.org/10.1016/B978-0-12-416041-5.00008-1.
(56) Percival, S. L.; Williams, D. W. Chapter Six - Escherichia Coli. In *Microbiology of Waterborne Diseases (Second Edition)*; Percival, S. L., Yates, M. V., Williams, D. W., Chalmers, R. M., Gray, N. F., Eds.; Academic Press: London, 2014; pp 89–117. https://doi.org/10.1016/B978-0-12-415846-7.00006-8.
(57) Buffers http://butane.chem.uiuc.edu/cyerkes/chem102aefa07/lecture_notes_102/lecture%2026-102.htm (accessed Jun 5, 2019).
(58) Phosphate buffered saline, used in diagnostic assay manufacturing | Sigma-Aldrich https://www.sigmaaldrich.com/catalog/product/sigma/p4417?lang=es&region=MX (accessed Jun 5, 2019).
(59) 10X Immuno Wash Buffer | Diagnostic BioSystems - Immunohistochemistry, Primary Antibodies, Monoclonal Antibodies, Polyclonal Antibodies, FITC, Antibodies, Automated Staining Instrumentation, Mouse and Rabbit Detection Systems, MultiPlex Kits, Ancillaries,

Chromogens, Special Stains, Literature http://dbiosys.com/2016/01/05/10x-immuno-wash-buffer-905/ (accessed Jun 5, 2019).
(60) Giddings, T. H.; Meehl, J. B.; Pearson, C. G.; Winey, M. Chapter 6 - Electron Tomography and Immuno-Labeling of Tetrahymena Thermophila Basal Bodies. In *Methods in Cell Biology*; Müller-Reichert, T., Ed.; Academic Press, 2010; Vol. 96, pp 117–141. https://doi.org/10.1016/S0091-679X(10)96006-8.
(61) BioTek: Fluorescence Intensity https://www.biotek.com/products/detection-fluorescence-intensity-technology.html (accessed May 30, 2019).
(62) BioTek: Time Resolved Fluorescence https://www.biotek.com/products/detection-time-resolved-fluorescence-technology.html (accessed May 30, 2019).
(63) Edwin Johan Ortiz Riaño. Desactivación de Fluoresceina Como Principio de Biodetección de Proteínas, Centro de Investigaciones en Óptica: León, Gto., México, 2018.
(64) Dunn, J.; Wild, D. Chapter 3.6 - Calibration Curve Fitting. In *The Immunoassay Handbook (Fourth Edition)*; Wild, D., Ed.; Elsevier: Oxford, 2013; pp 323–336. https://doi.org/10.1016/B978-0-08-097037-0.00022-1.
(65) Thompson, M.; Ramsey, M. H. Environmental and Agricultural Applications of Atomic Spectroscopy*. In *Encyclopedia of Spectroscopy and Spectrometry (Second Edition)*; Lindon, J. C., Ed.; Academic Press: Oxford, 1999; pp 494–501. https://doi.org/10.1016/B978-0-12-374413-5.00135-4.
(66) Indrayanto, G. Chapter Five - Validation of Chromatographic Methods of Analysis: Application for Drugs That Derived From Herbs. In *Profiles of Drug Substances, Excipients and Related Methodology*; Brittain, H. G., Ed.; Academic Press, 2018; Vol. 43, pp 359–392. https://doi.org/10.1016/bs.podrm.2018.01.003.
(67) Bhalla, N.; Jolly, P.; Formisano, N.; Estrela, P. Introduction to Biosensors. *Essays Biochem.* **2016**, *60* (1), 1. https://doi.org/10.1042/EBC20150001.
(68) Sharpe, A. N.; Jackson, A. K. Stomaching: A New Concept in Bacteriological Sample Preparation. *Appl. Microbiol.* **1972**, *24* (2), 175–178.
(69) Findlay, J. W. A.; Smith, W. C.; Lee, J. W.; Nordblom, G. D.; Das, I.; DeSilva, B. S.; Khan, M. N.; Bowsher, R. R. Validation of Immunoassays for Bioanalysis: A Pharmaceutical Industry Perspective. *J. Pharm. Biomed. Anal.* **2000**, *21* (6), 1249–1273. https://doi.org/10.1016/S0731-7085(99)00244-7.
(70) Selvarajah, S.; Negm, O. H.; Hamed, M. R.; Tubby, C.; Todd, I.; Tighe, P. J.; Harrison, T.; Fairclough, L. C. Development and Validation of Protein Microarray Technology for Simultaneous Inflammatory Mediator Detection in Human Sera. *Mediators Inflamm.* **2014**, *2014*, 820304–820304. https://doi.org/10.1155/2014/820304.

A. Appendix I

Index of figures of Appendix I

Index of tables of Appendix I

Section 1. Ab-QD optimization

All the *E. coli* samples presented in this section are measured in CFU mL^{-1}, and the elapsed time mentioned are measured in minutes. The volume used for all the assays were 100µL of sample adding 100µL of probe.

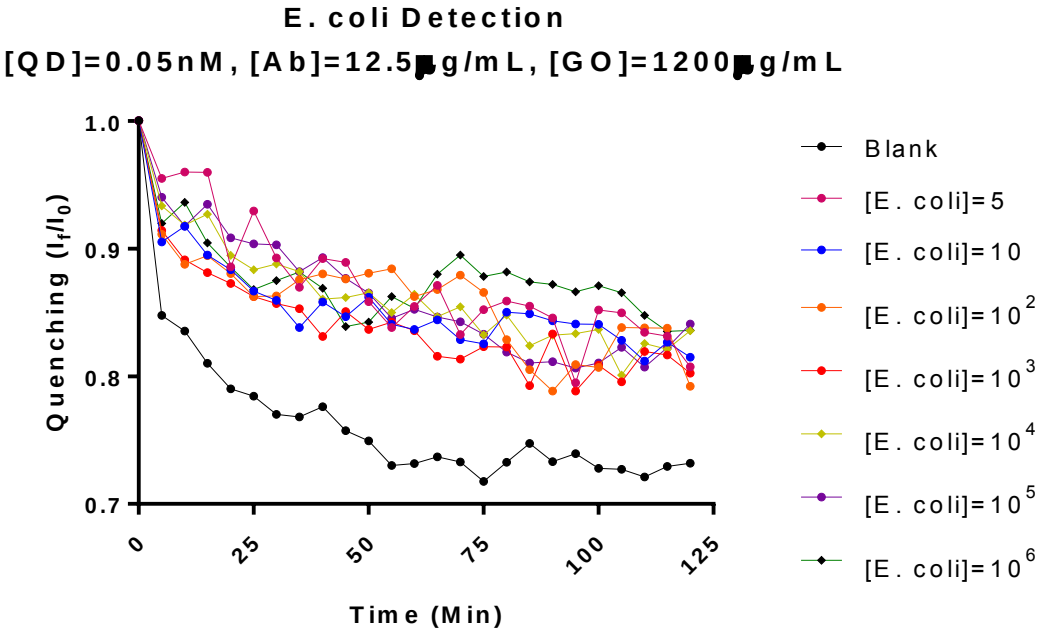

Figure. A. Ab-QD optimization. E. coli detection kinetic with [QD]=0.05nM, [Ab]=12.5µg mL^{-1}. Date of identification: 180503.

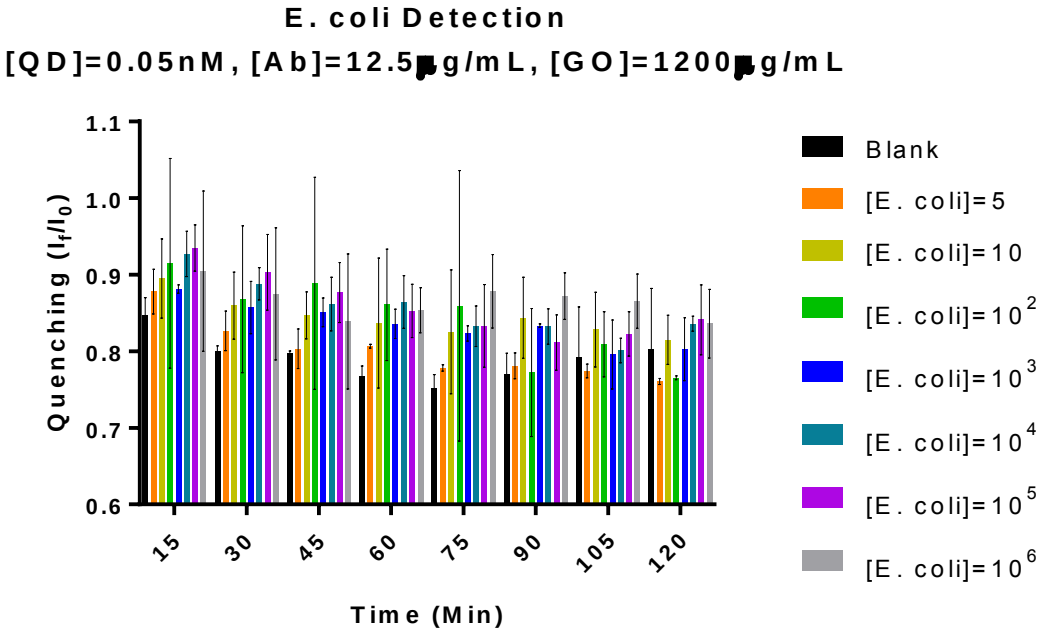

Figure. B. Ab-QD optimization. E. coli detection bar chart with [QD]=0.05nM, [Ab]=12.5µg mL^{-1}. Date of identification: 180503.

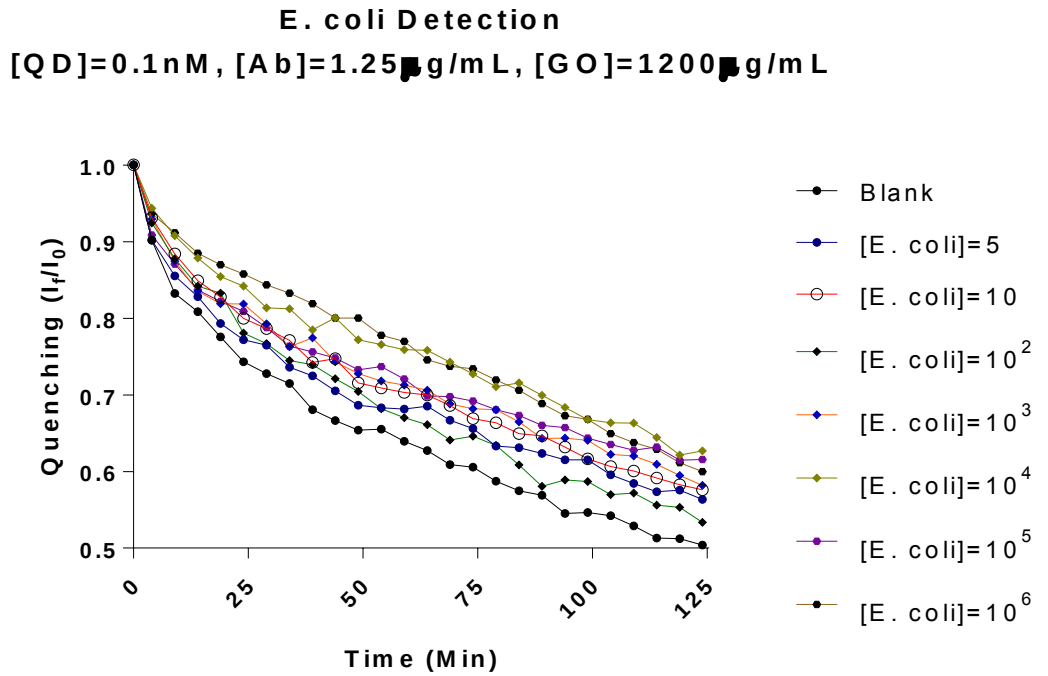

Figure. C. Ab-QD optimization. E. coli detection kinetic with [QD]=0.1nM, [Ab]=1.25µg mL-^{1}. Date of identification: 180509.

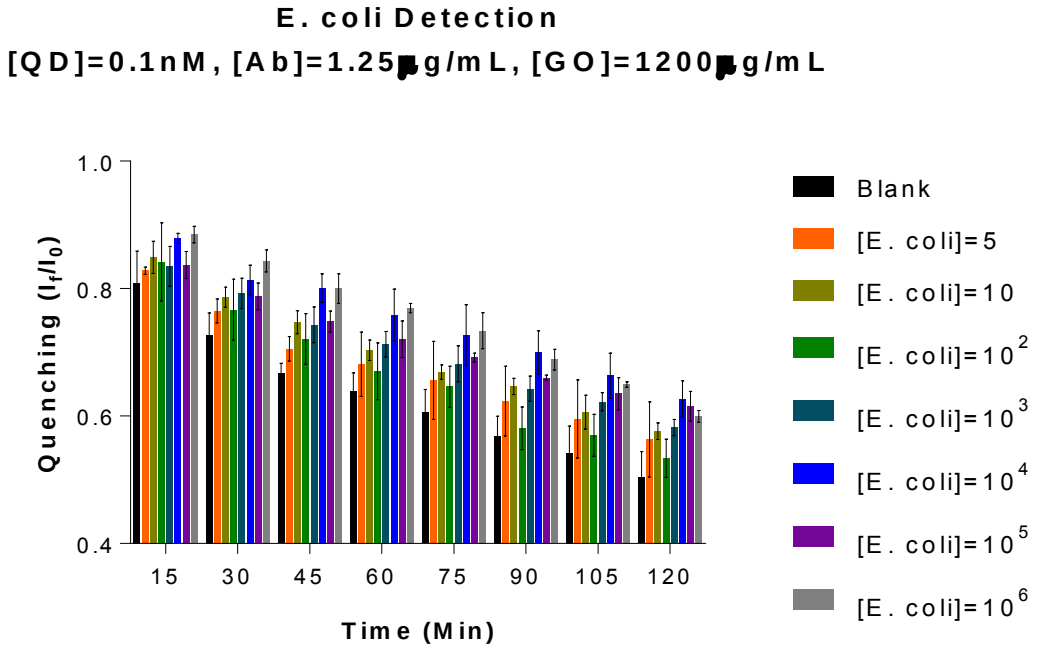

Figure. D. Ab-QD optimization. E. coli detection bar chart with [QD]=0.1nM, [Ab]=1.25µg mL^{-1}. Date of identification: 180509.

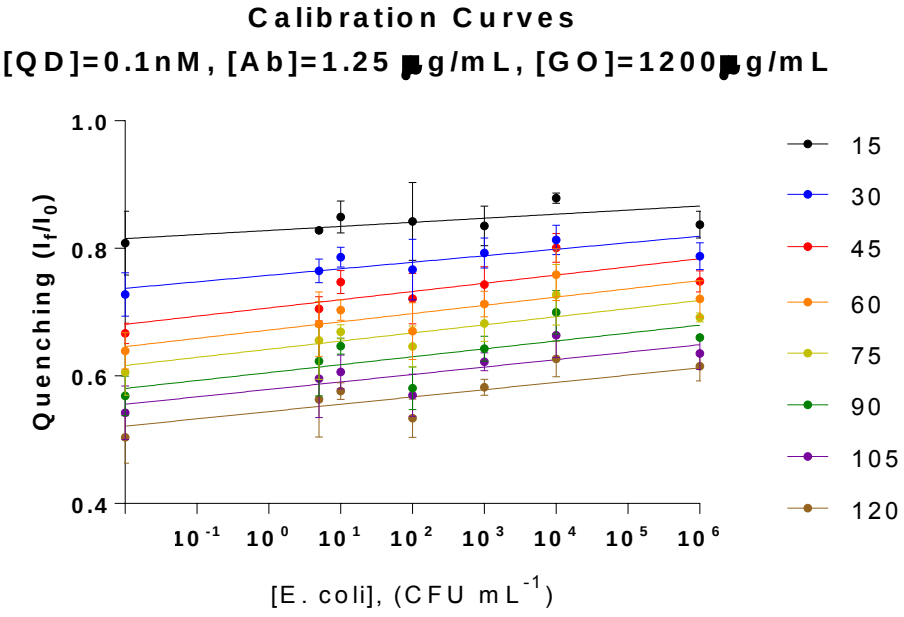

Figure. E. Ab-QD optimization. Calibration curve for [QD]=0.1nM, [Ab]=1.25µg mL^{-1}. Date of identification: 180509.

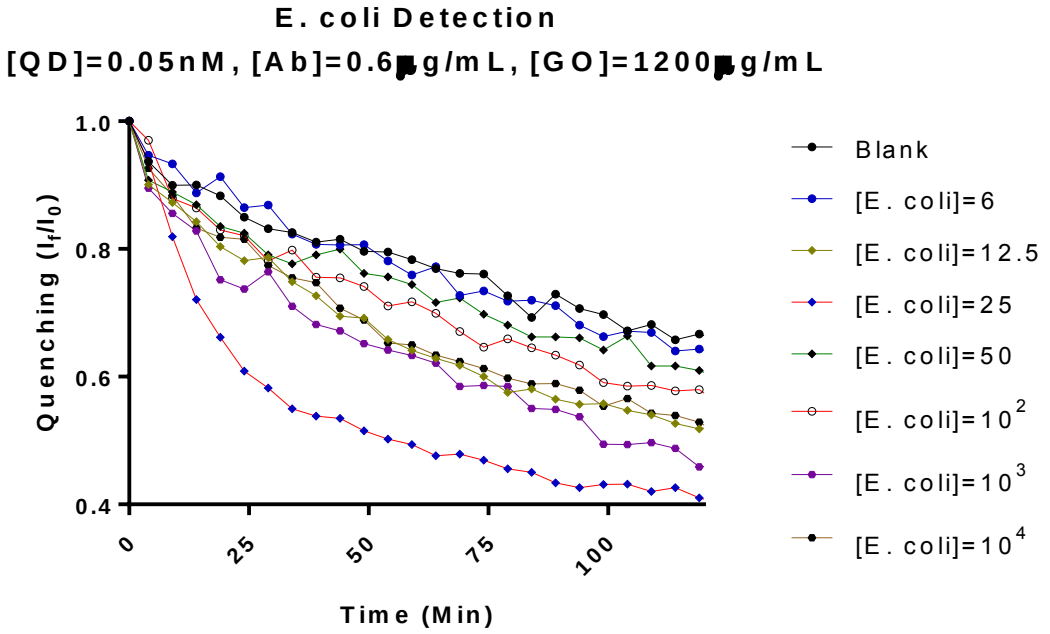

Figure. F. Ab-QD optimization. E. coli detection kinetic with [QD]=0.05nM, [Ab]=0.6µg mL-1. Date of identification: 180704.

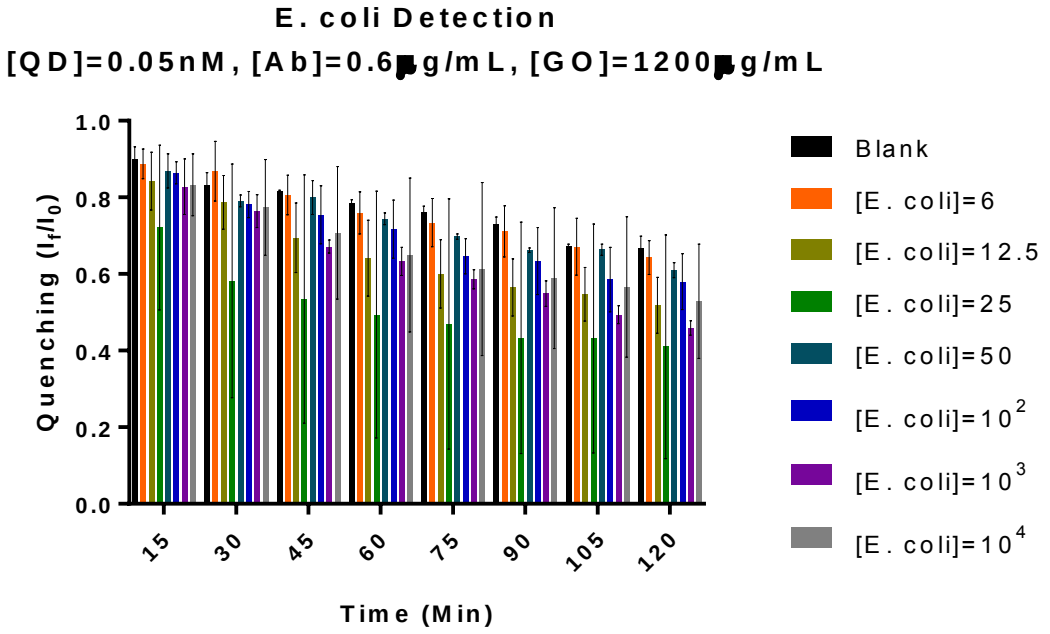

Figure. G. Ab-QD optimization. E. coli detection bar chart with [QD]=0.05nM, [Ab]=0.6µg mL-1. Date of identification: 180704.

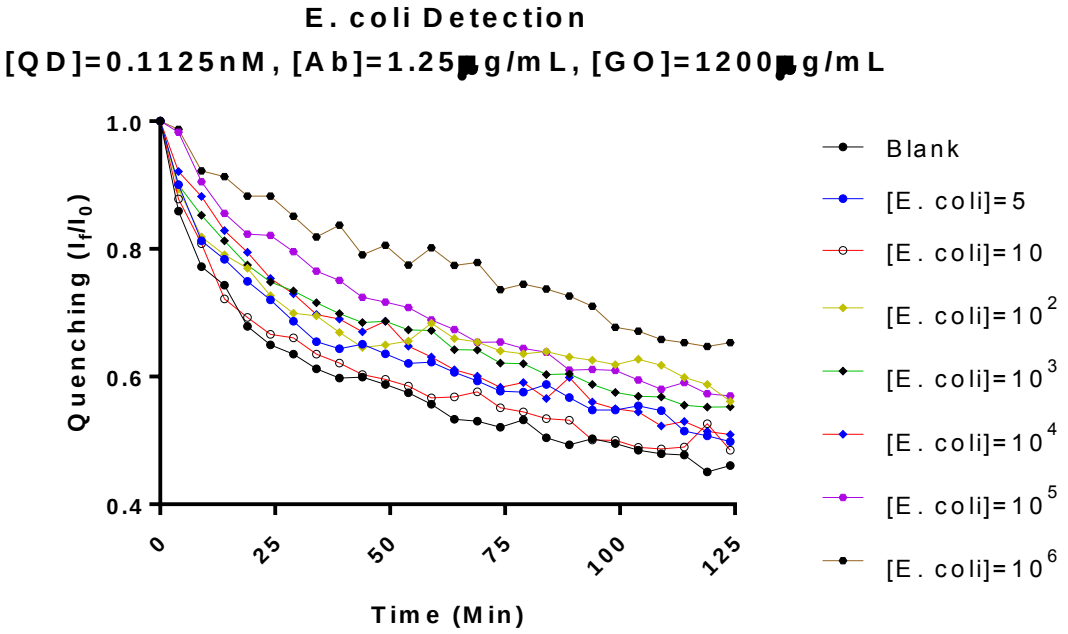

Figure. H. Ab-QD optimization. E. coli detection kinetic with [QD]=0.1125nM, [Ab]=1.25µg mL^{-1}. Date of identification: 181003.

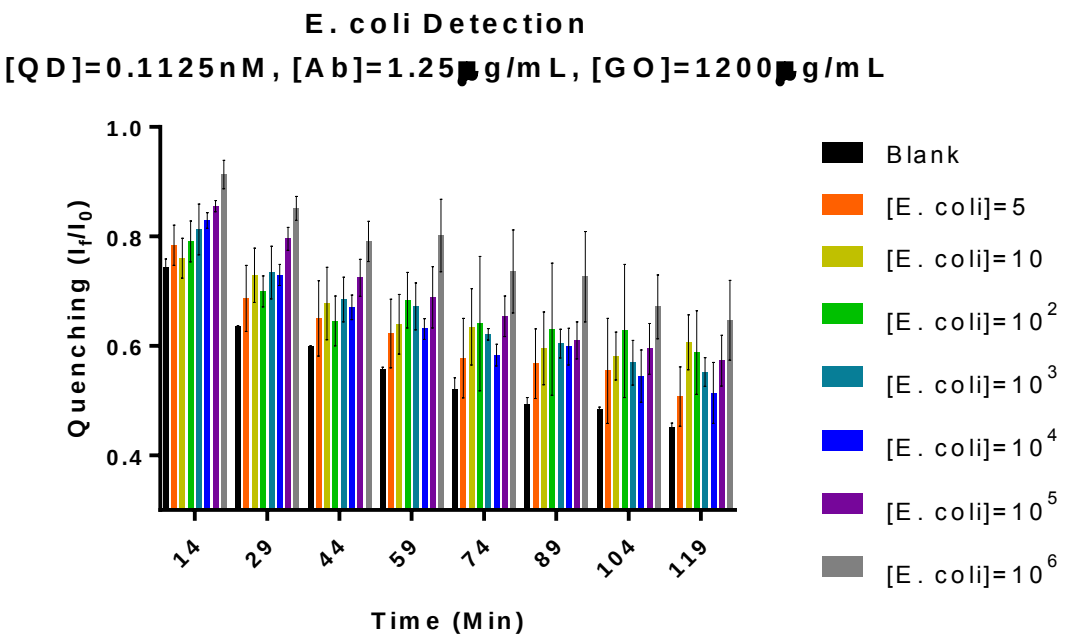

Figure. I. Ab-QD optimization. E. coli detection bar chart with [QD]=0.1125nM, [Ab]=1.25µg mL^{-1}. Date of identification: 181003.

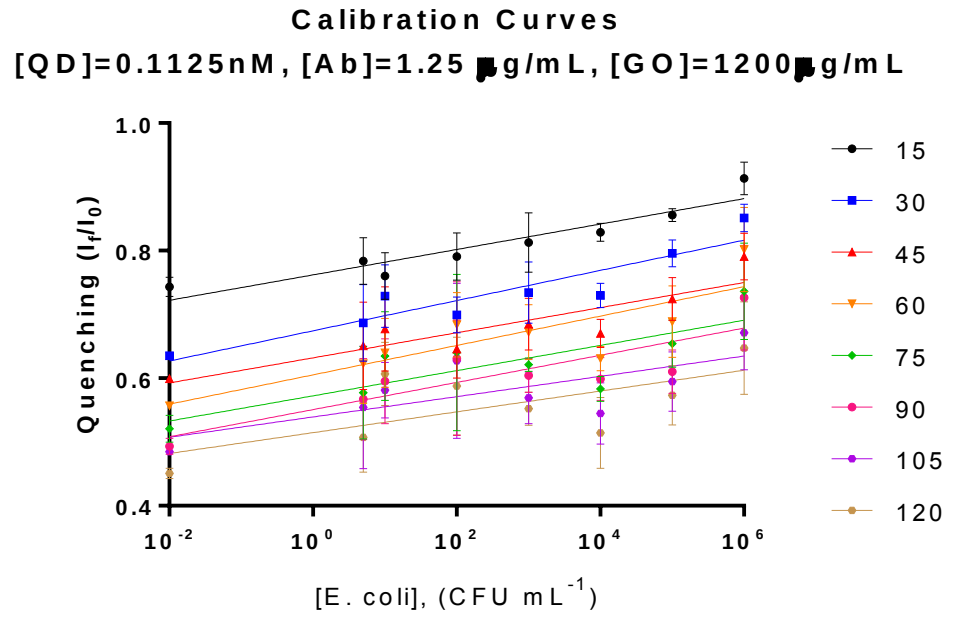

Figure. J. Ab-QD optimization. Calibration curve for [QD]=0.1125nM, [Ab]=1.25µg mL^{-1}. Date of identification: 181003.

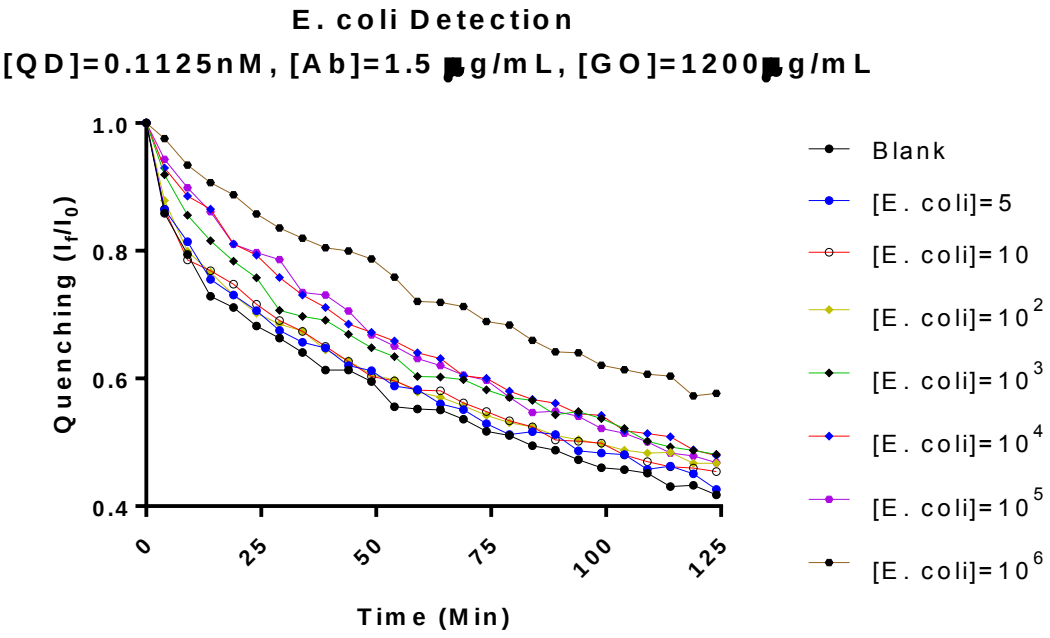

Figure. K. Ab-QD optimization. E. coli detection kinetic with [QD]=0.1125nM, [Ab]=1.5µg mL^{-1}. Date of identification: 181017.

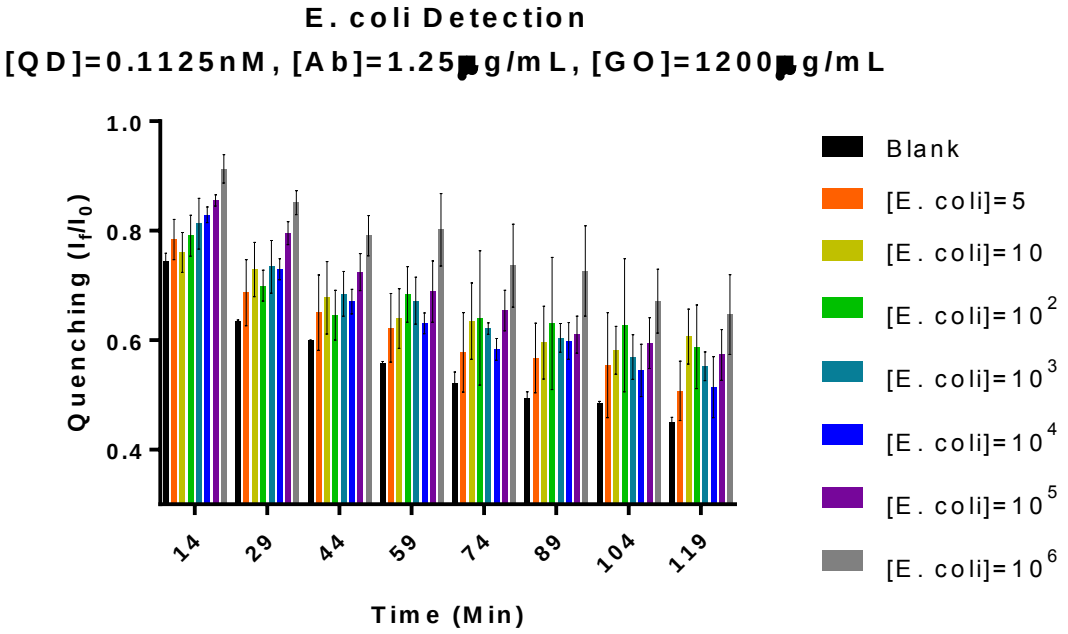

Figure. L. Ab-QD optimization. E. coli detection bar chart with [QD]=0.1125nM, [Ab]=1.25μg mL^{-1}. Date of identification: 181017.

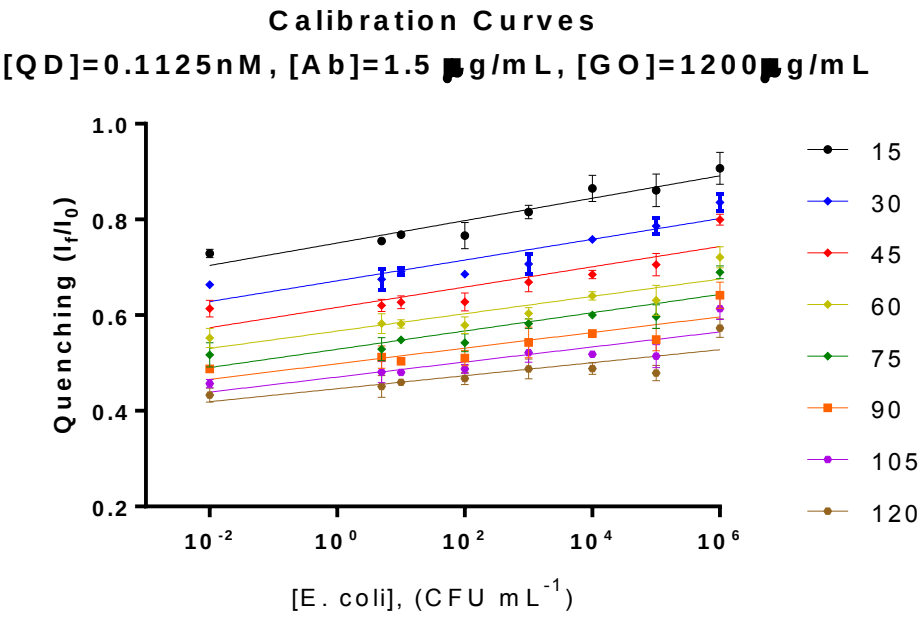

Figure. M. Ab-QD optimization. Calibration curve for [QD]=0.1125nM, [Ab]=1.5μg mL^{-1}. Date of identification: 181017.

Section 2. Coefficient of variation

Table. A. Coefficient of variation of every sample examined. All the assays presented in this table were perform with [GO]=1200 µg mL^{-1} and [QD]=0.1125nM. The first column gives information about the date identification of the assay.

Date aammdd	**Ab (µg mL^{-1})**	**Time (Min)**	**R^2**	**1/slope**	**LOD (CFU mL^{-1})**	**Sample examined (CFU mL^{-1})**	**CV (SD/m) *100**
181017	0.9	15	0.9214	42.37	143.21	0	2.11594167
						5	3.66470251
						10	0.38956052
						10^2	3.26170469
						10^3	3.33934469
						10^4	9.63409754
						10^5	2.67108644
						10^6	3.15422147
181017	***0.9***	***30***	***0.8686***	***40.74***	***1.81***	0	**0.49415331**
						5	2.30899729
						10	2.57384151
						10^2	1.22421309
						10^3	3.93495401
						10^4	**6.42905468**
						10^5	2.53979124
						10^6	3.8523104
181003	1.25	15	0.9343	40.76	16557.69	0	2.05760265
						5	4.69314975
						10	4.7933145
						10^2	4.72565726
						10^3	5.70817051
						10^4	1.7269474
						10^5	1.18519658
						10^6	2.83059339
181003	1.25	30	0.8385	35.56	210.37	0	0.26816284
						5	8.76601685
						10	6.77732673
						10^2	4.01898673
						10^3	6.5654719
						10^4	2.63870699
						10^5	2.64250627
						10^6	2.5674514
181017	1.5	15	0.9596	34.68	8.22	0	1.27929303
						5	1.0177269
						10	0.43498454
						10^2	3.60710332
						10^3	1.7048298

						10^4	3.1514035
						10^5	3.97183835
						10^6	3.68154262
181017	1.5	30	0.93	36.44	14.28	0	0.95882266
						5	3.17645198
						10	1.190657
						10^2	0.77314275
						10^3	3.00922573
						10^4	0.76992226
						10^5	2.18456423
						10^6	2.23224185

Section 3. Inter-assay coefficient of variation

Table. B. Inter assay accuracy. Coefficient of variation calculated for every moment measured. The E. coli sample used for the calculation were in a concentration of 10^3CFU mL^{-1}.

Assay	Time (Min)	Mean blank sample	Mean *E. coli* sample	SD blank sample	SD *E. coli* sample	CV (%) blank sample	CV (%) *E. coli* sample
181017	15	0.76225799	0.82628786	0.03539332	0.02477088	3.41618205	2.9978511
	30	0.6759135	0.74618147	0.04665072	0.02647479	5.60046705	3.54803575
	45	0.61819635	0.68651587	0.04465089	0.03213375	4.38113393	4.68070011
190312	60	0.56621984	0.64447797	0.05125031	0.03002873	5.19733295	4.65938831
	75	0.5357704	0.58810958	0.03343761	0.03335255	4.08708368	5.67114568
	90	0.49332203	0.55761233	0.03412544	0.01937797	4.46688809	3.4751693
190311	105	0.47675648	0.53696105	0.03064398	0.02776888	3.87674947	5.17148824
	120	0.44277618	0.50519547	0.03342515	0.02256664	5.61853293	4.46691159

Section 4. Real sample test

All the real sample tests were made with the parameters defined as optimal. [GO]=1200 µg mL^{-1}, [Ab]= 0.9 µg mL^{-1}, [QD]0.1125nM, orbital agitation, volume: 100µL of sample adding 100µL of probe.

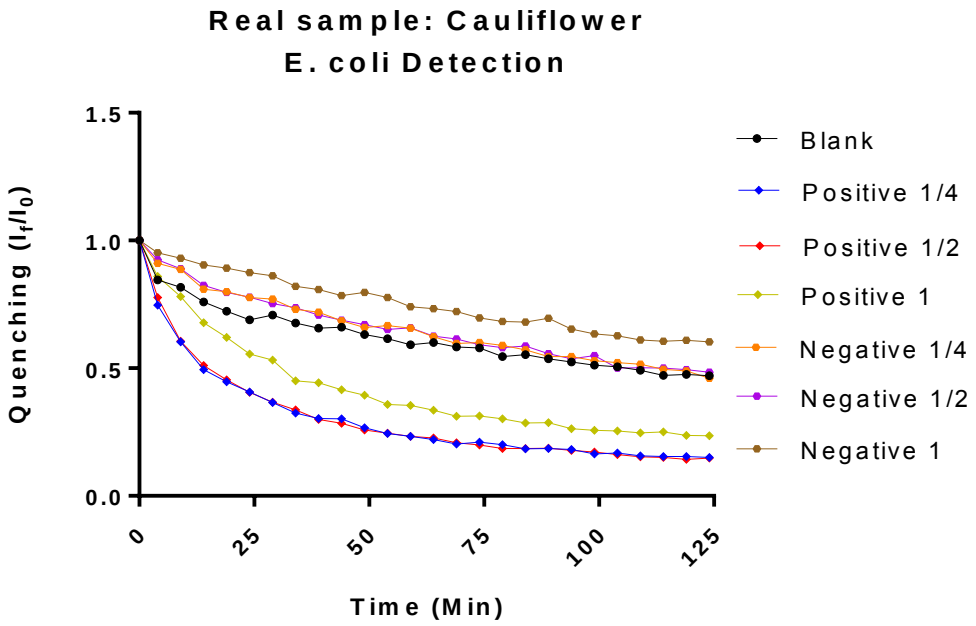

Figure. N. Kinetic of real sample: Cauliflower. Samples diluted in 1, 1/2, 1/4 (v/v)

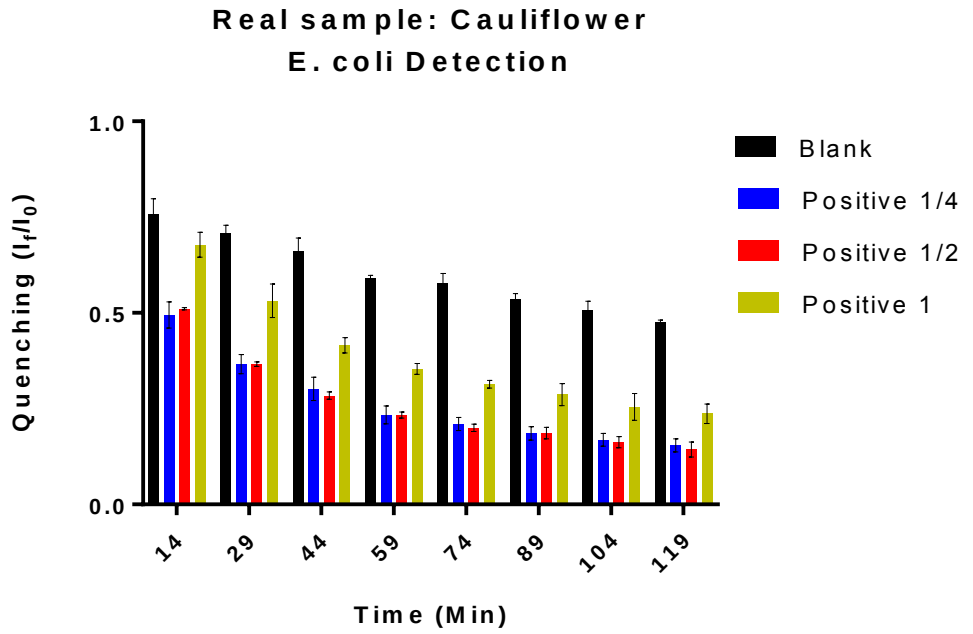

Figure. O. Bar chart of real sample: Cauliflower. Samples reported as E. coli positive diluted in 1, 1/2, 1/4 (v/v)

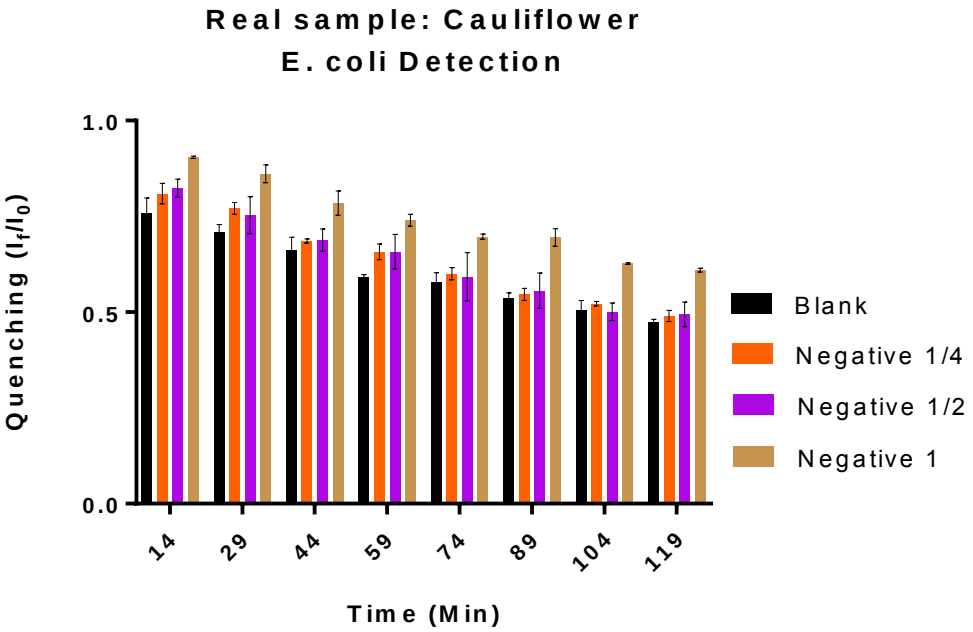

Figure. P. Bar chart of real sample: Cauliflower. Samples reported as E. coli negative diluted in 1, 1/2, 1/4 (v/v)

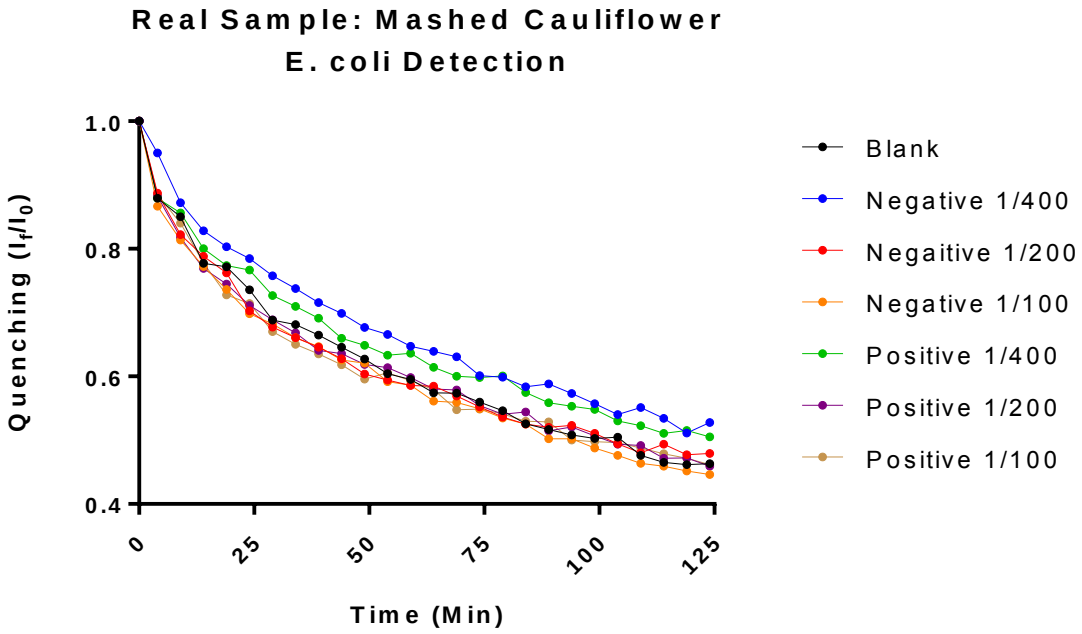

Figure. Q. Kinetic of real sample: Cauliflower. Samples diluted in 1/100, 1/200, 1/400 (v/v)

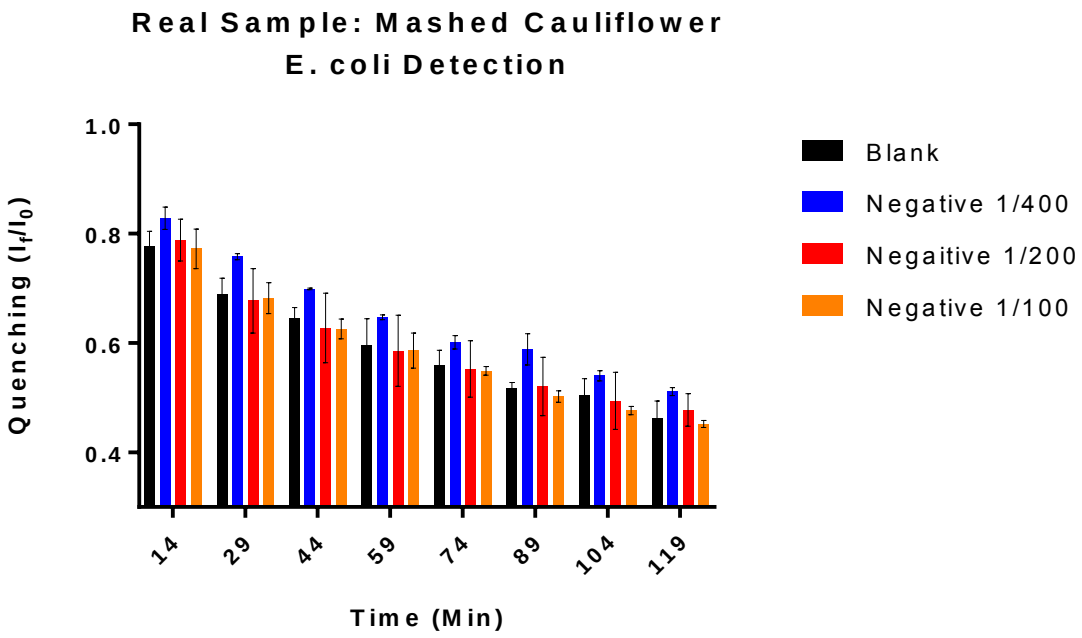

Figure. R. Bar chart of real sample: Cauliflower. Samples reported as E. coli negative diluted in 1/100, 1/200, 1/400 (v/v)

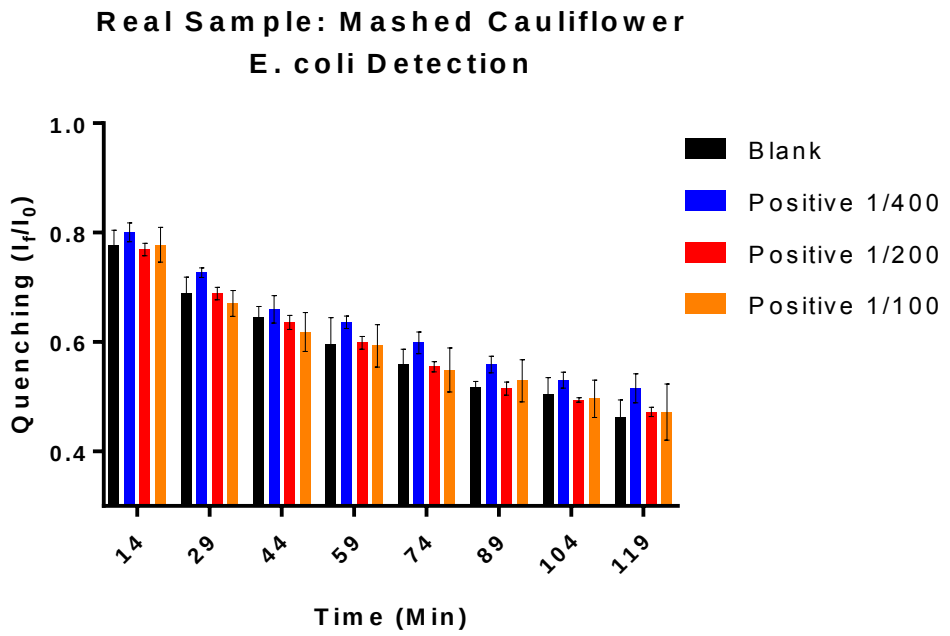

Figure. S. Bar chart of real sample: Cauliflower. Samples reported as E. coli positive diluted in 1/100, 1/200, 1/400 (v/v)

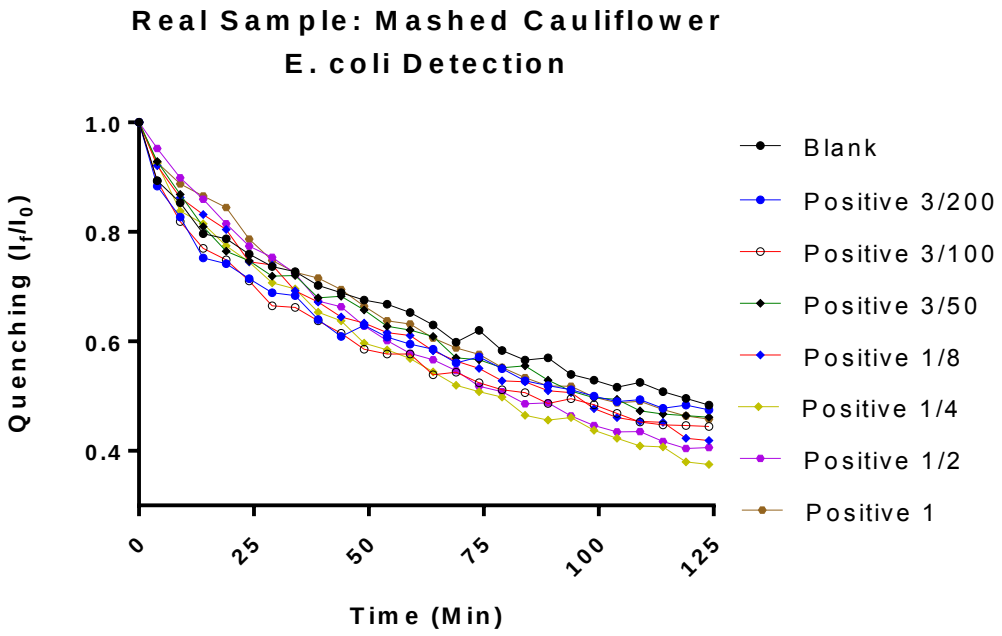

Figure. T. Kinetic of real sample: Cauliflower. Samples reported as E. coli positives diluted in 1, 1/2, 1/4, 1/8, 3/50, 3/100, 3/200 (v/v)

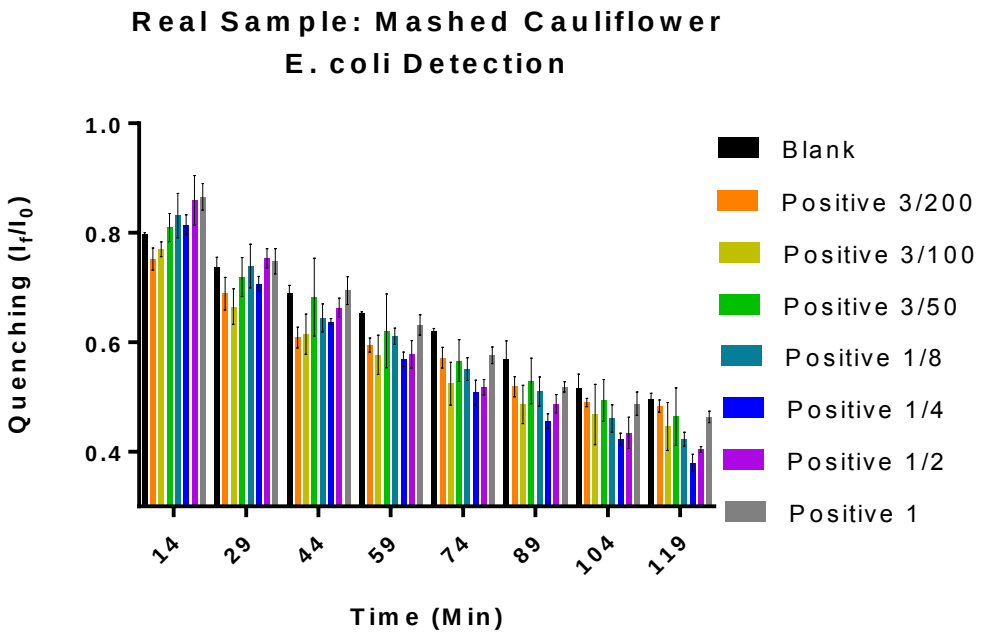

Figure. U. Bar chart of real sample: Cauliflower. Samples reported as E. coli positives diluted in 1, 1/2, 1/4, 1/8, 3/50, 3/100, 3/200 (v/v)

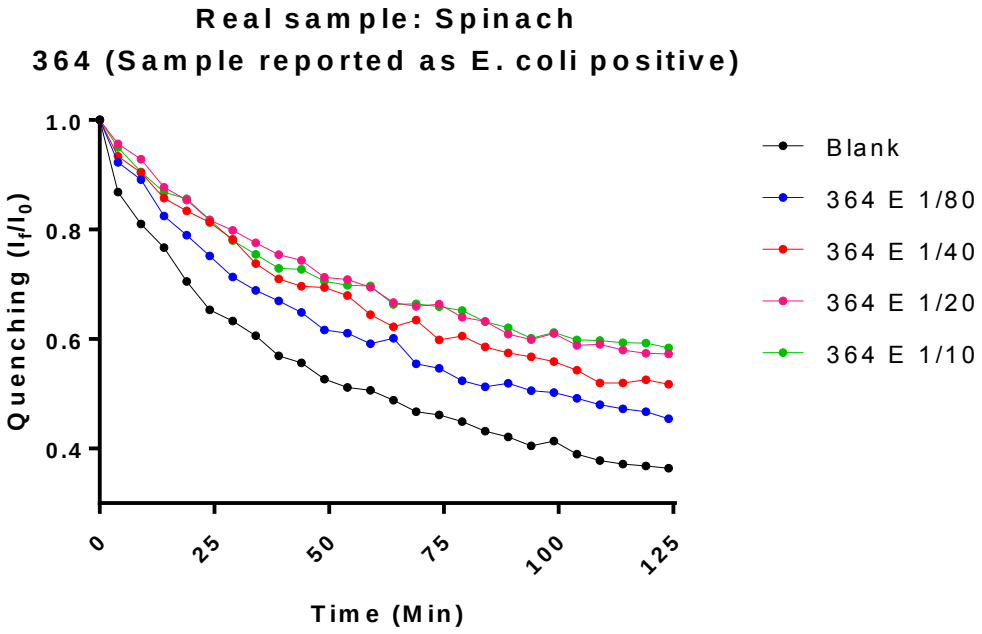

Figure. V. Kinetic of real sample: Spinach. Samples reported as E. coli positives diluted in 1/10, 1/20, 1/40, 1/80 (v/v).

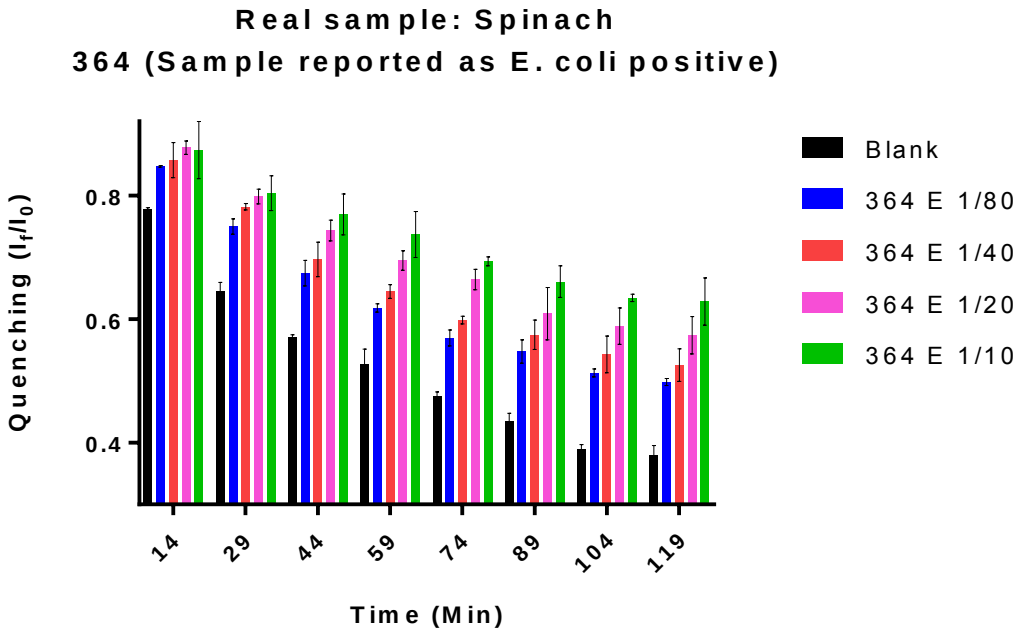

Figure. W. Bar chart of real sample: Spinach. Samples reported as E. coli positives diluted in 1/10, 1/20, 1/40, 1/80 (v/v).

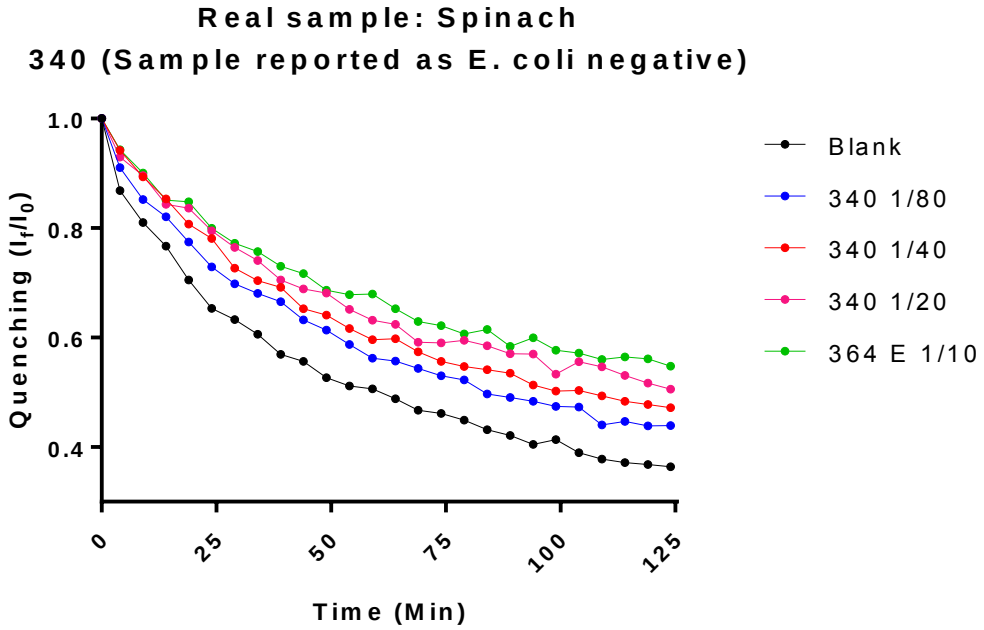

Figure. X. Kinetic of real sample: Spinach. Samples reported as E. coli negatives diluted in 1/10, 1/20, 1/40, 1/80 (v/v).

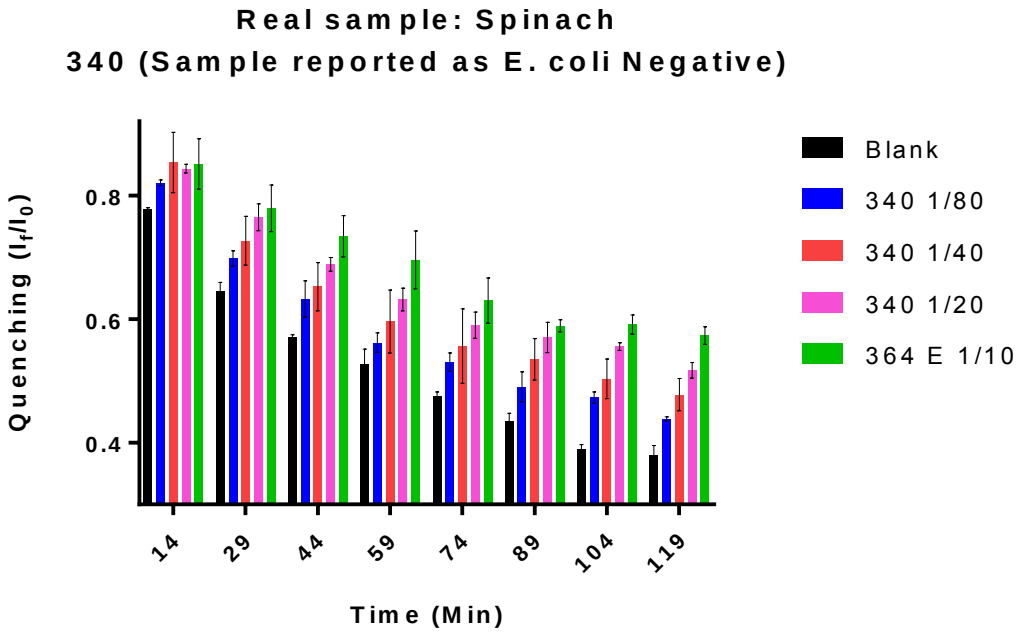

Figure. Y. Bar chart of real sample: Spinach. Samples reported as E. coli negatives diluted in 1/10, 1/20, 1/40, 1/80 (v/v).

Section 5. Cost estimation

Table. C. Cost estimation per test in MXN

Material	Total volume	Concentration	Cost	Volume per assay	Used concentration	Cost per assay
Microwell plate	96 wells	N/A	$ 102.08	3 wells	N/A	$ 3.19
GO	1000 mL	5000 µg mL^{-1}	$ 3,700.00	26.4 µL	1200 µg mL^{-1}	$ 0.1
Ab	500 µL	4000 µg mL^{-1}	$ 12,000.00	0.07 µL	0.9 µg mL^{-1}	$ 1.68
QD	200 µL	1 µM	$ 13,000.00	0.034 µL	0.1125 nM	$ 2.21
PBS	100 tablets	N/A	$ 2,420.00	N/A	N/A	$ 0.2
BSA	25 g	N/A	$17,720.00	N/A	N/A	$ 0.6
Tween 20	100 mL	N/A	$720.00	N/A	N/A	$ 0.1
					TOTAL	$ 8.08

Note: Complete assay is considered as a parallel experiment with 3 wells, that is $2.69 MXN per well

Table. D. Table of comparison of costs and LOD of the different methods to determine E. coli

Method	Range LOD (CFU mL^{-1})	Cost per test in MXN
Proposed biosensing platform	1.8	$8.08
ELISA	From 6.25 x 10^3 to 4 x 10^5	$95.00
Culture-based assay	1	$65.00